

Session 7: Design of connections

Objektyp: **Group**

Zeitschrift: **IABSE reports = Rapports AIPC = IVBH Berichte**

Band (Jahr): **75 (1996)**

PDF erstellt am: **23.06.2024**

Nutzungsbedingungen

Die ETH-Bibliothek ist Anbieterin der digitalisierten Zeitschriften. Sie besitzt keine Urheberrechte an den Inhalten der Zeitschriften. Die Rechte liegen in der Regel bei den Herausgebern.

Die auf der Plattform e-periodica veröffentlichten Dokumente stehen für nicht-kommerzielle Zwecke in Lehre und Forschung sowie für die private Nutzung frei zur Verfügung. Einzelne Dateien oder Ausdrucke aus diesem Angebot können zusammen mit diesen Nutzungsbedingungen und den korrekten Herkunftsbezeichnungen weitergegeben werden.

Das Veröffentlichen von Bildern in Print- und Online-Publikationen ist nur mit vorheriger Genehmigung der Rechteinhaber erlaubt. Die systematische Speicherung von Teilen des elektronischen Angebots auf anderen Servern bedarf ebenfalls des schriftlichen Einverständnisses der Rechteinhaber.

Haftungsausschluss

Alle Angaben erfolgen ohne Gewähr für Vollständigkeit oder Richtigkeit. Es wird keine Haftung übernommen für Schäden durch die Verwendung von Informationen aus diesem Online-Angebot oder durch das Fehlen von Informationen. Dies gilt auch für Inhalte Dritter, die über dieses Angebot zugänglich sind.



SESSION 7
DESIGN OF CONNECTIONS

Leere Seite
Blank page
Page vide



Component Method Validation Tests in Precast Concrete Semi-Rigid Connections

Kim S ELLIOTT
Gwynne DAVIES
Halil GÖRGÜN

Department of Civil Engineering
University of Nottingham, UK

Drs Elliott (b 1953) and Davies (b 1935) are Senior Lecturer and Reader, respectively in Structural Eng. Mr Görgün (b 1963) is a Research Student studying towards a PhD in this work. Drs Elliott and Davies have supervised some 8 projects in precast structures.

Summary

Full scale testing of a symmetrical precast concrete beam-column connection has been carried out to generate semi-rigid moment-rotation ($M-\phi$) data which may be compared with that obtained using the *component method*. In this way the deformabilities of isolated, small scale compression and tension joints, representing the bottom and top fibres of a full scale test, are summed to generate $M-\phi$ curves. The points where the stiffness of the full scale connection changes, and the magnitude of the connection stiffness are faithfully reproduced by the component method, but the ultimate test moment and rotation capacity are not. This is because little redistribution of flexural stress is possible in isolated tests, and cracking is affected by the presence of floor slabs in the full scale tests. Within these limitations the component method provides a reasonable tool to generate $M-\phi$ data.

1. Background to Semi-rigid Connection Testing

Precast concrete skeletal frames are designed as braced, unbraced or partially braced structures, in which the columns are usually continuous at the floor level connections, as shown in Fig. 1, where a solid steel billet is awaiting a third beam at an internal connection. The majority of connections however are either single sided (at the edges of buildings) or double sided (at interior columns), and these have formed the basis for all the experimental tests carried out to date. Precast connections are also distinguished between those which include floor slabs (usually hollow cored units) spanning perpendicular to the plane of the beam, and those which do not. In the former, the tie steel at the ends of the floor slabs are an integral part of the stability ties required by most Codes of Practice, and form a vital component of the connection.

Mahdi (1,2) established that the most common types of connection exhibit some degree of in-plane flexural semi-rigidity. Values of strength, stiffness and ($M-\phi$) data have been given previously (1). Of course, it rests with the design engineer to decide whether this information justifies a semi-rigid frame design. However, the need to provide further $M-\phi$ data, without incurring the additional expense of testing, has led to the development of the so called *component method* (3,4). Here $M-\phi$ data are generated by superposition of individual (and combined) actions within the connection. The component method is accepted in semi-rigid steel connection analysis, and previous work by the authors (4) suggested that it might also be feasible in precast concrete connections.

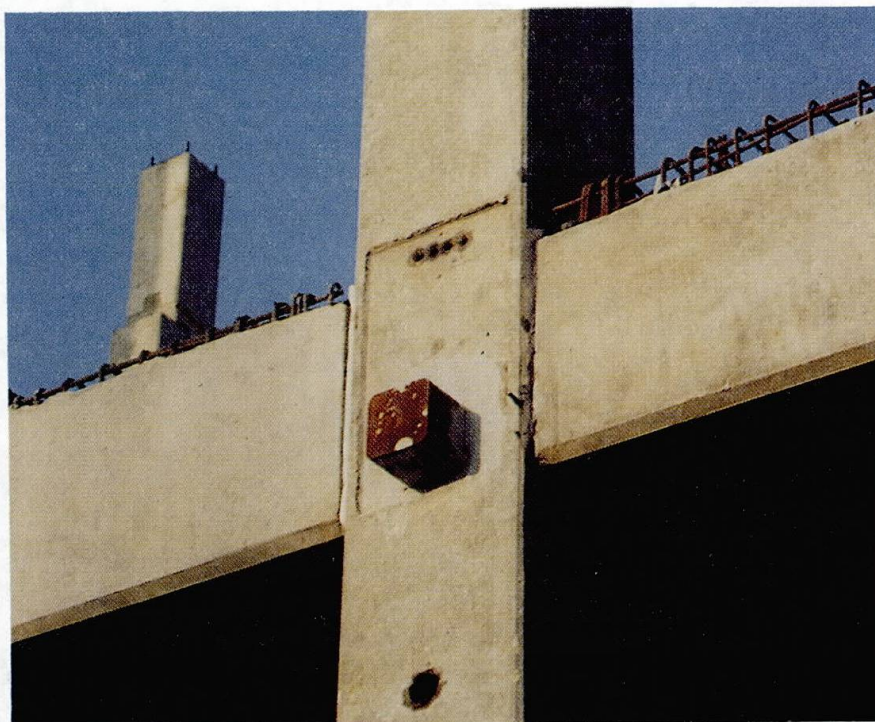


Fig. 1. Three-way precast concrete billet type connector. Note the projecting interface stirrups in the beams and the sleeves in the column to receive continuity tie steel.

This present work takes the above a further step forward by determining the $M-\phi$ curves for a double sided connection, subjected to equal hogging moments and shear forces, by three methods:

1. direct measurement by full scale testing (called 'Method 1');
2. joint deformations measured and computed in a full scale test (called 'Method 2');
3. joint deformations measured in isolated tests and computed according to the 'Component Method'.

2. Full Scale Experimental Tests

2.1 Design of Test Specimens and Test Procedure

Details of the cruciform test assembly are given in Fig. 2. This is essentially a symmetrical beam-column connection, with proprietary slip formed hollow cored floor slabs (supplied by Bison Floors, UK). The length of the beams, and hence the position of the bending load P (Fig. 2[a]), was selected to represent the point of contraflexure in a uniformly distributed loaded beam of about 12 m span. Assuming that the maximum bending moment is recorded at the face of the column, the shear span / beam effective depth ratio for the load is $2365 / 450 = 5.25$. The effective depth to the reinforcement is $500 - 50 = 450$ mm.

The 200 kN (vertical shear rated) beam - column connector is of the *welded plate* type, comprising a 100 x 100 mm solid steel column billet (Figs. 1 and 3) fillet welded (20 mm leg length x 80 mm long) to a 25 mm thick vertical plate cast into the beam. The 100 mm gap at the end of the beam was filled with 10 mm aggregate insitu concrete (nominal $f_{cu} = 40$ N/mm²) up to the top level of the beam.

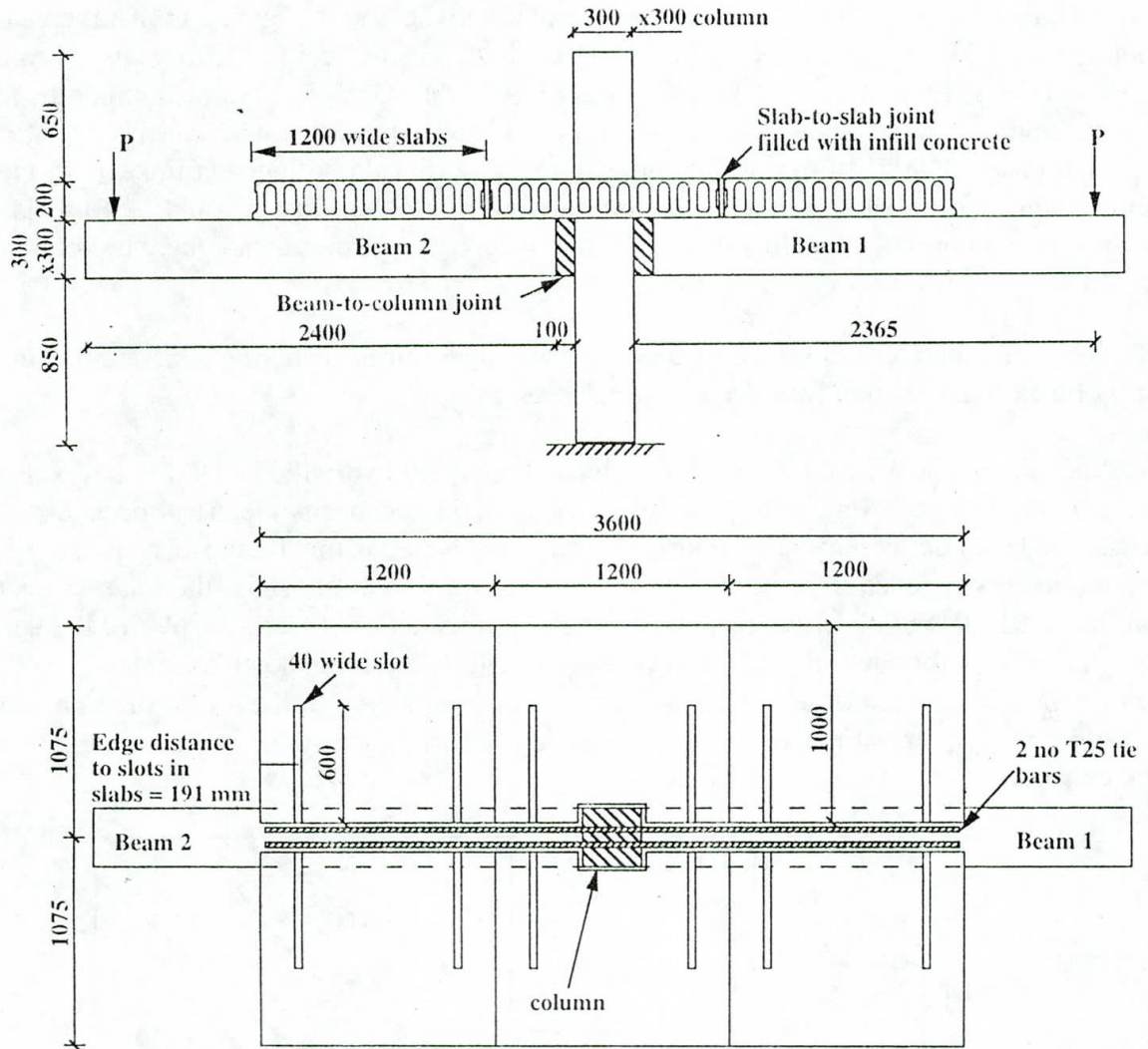


Fig. 2. Arrangement of full scale precast concrete connection test. (a) Elevation (b) Plan.

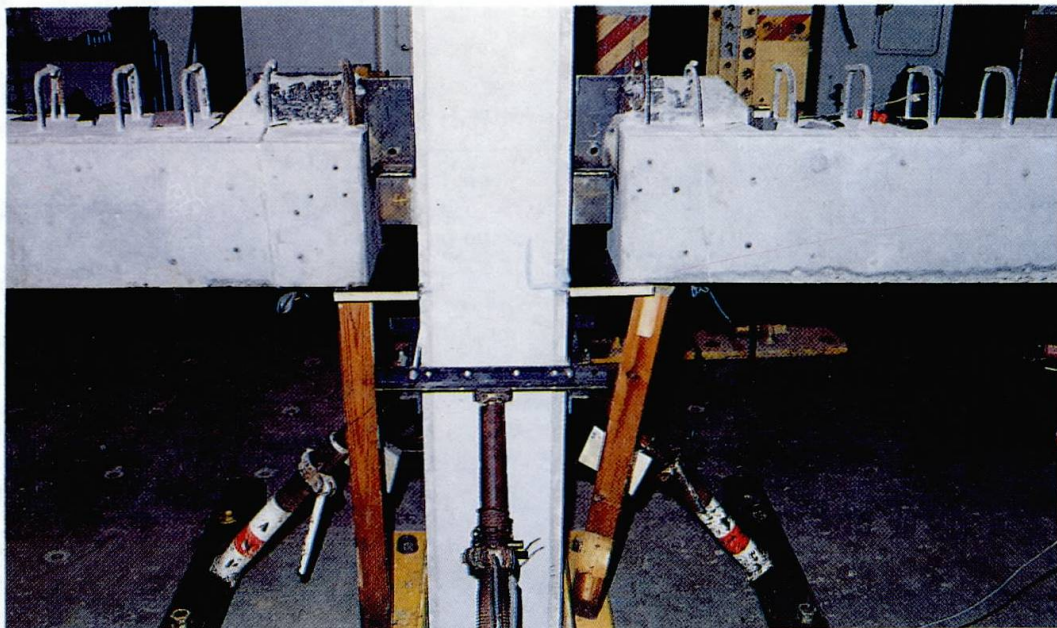


Fig. 3. Construction of connector in laboratory.



The precast floor slabs were concreted into position using 10 mm aggregate insitu concrete (nominal $f_{cu} = 30 \text{ N/mm}^2$) after 12 mm diameter high tensile steel (T12, $f_y = 460 \text{ N/mm}^2$) tie bars were placed into the 40 mm wide milled slots in the slabs. The nominal strengths for the precast column and beams was $f_{cu} = 40 \text{ N/mm}^2$. Column reinforcement consisted of 4 no. T25 main bars and T 12 links at 185 mm centres. Additional confinement links at 75 mm centres were positioned adjacent to the billet. Beam reinforcement consisted of 4 no. T20 bars in the top and bottom, with T10 links at 100 mm centres. Further details may be found in reference 5.

The design moment of resistance of 235 kNm was determined using the concrete rectangular stress block method and unfactored material stresses.

Loading was applied incrementally through hand operated hydraulic jacks (the intervals of loading are evident in Fig. 6) and measured using 200 kN capacity electrical resistance load cells. The beam deflections shown in Fig. 4 were measured using a number of linear potentiometers attached to a rod which was bolted to the column. Thus, the relative rotation **and** the shear deflection of the beam to the column was deduced from the plot of the deflection shown in Fig. 4 for each increment of load (only selected values shown). Compressive deformations δ_b in the bottom of the beam, and crack widths δ_r in the top of the slab were measured using pairs of linear potentiometers, one either side of the beam to check for out-of-plane movements.

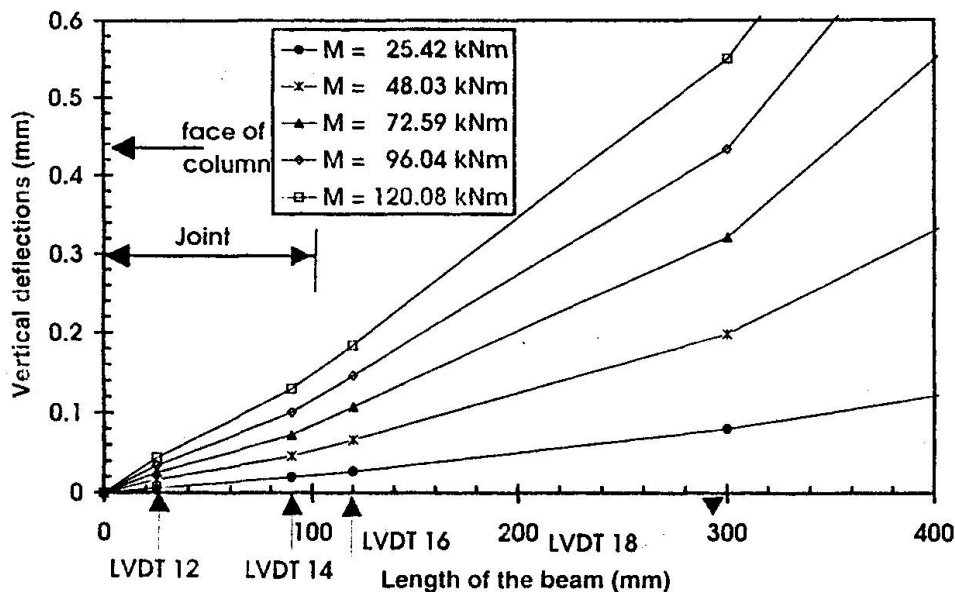


Fig. 4. Profiles of vertical beam deflections at selected values of applied bending moment.

2.2 Test Results

The $M-\phi$ data presented in Fig. 5 are average values for the mean results obtained for both Beams 1 and 2 (Fig. 2[a]). M_{cnn} refers to the applied hogging bending moment at the face of the column = $2.365 P$ (kNm units). The relative rotation ϕ refers to the **total** rotation of the beam relative to the column, and was determined using two methods:-

Method 1. By measurement of the gradient of the vertical deflection vs distance curves in Fig. 4 over a distance of 300 mm from the face of the column. Shear deflections are thus

eliminated. Fig. 4 also shows that the rotation in the joint region (up to 100 mm from the face of the column) is approximately two-thirds of the total beam-column rotation.

Method 2. By the addition of horizontal joint deformations in the bottom (δ_b) and top (δ_t) fibres of the connection divided by the total depth of the connection, i.e. $(\delta_b + \delta_t) / 500$ (mm units). This method assumes full shear interaction between the floor slab and the beam. The data for δ_b and δ_t are presented in Fig. 6, which shows that crack widths at the top of the slab are some five times greater than the compressive deformations in the beam.

Fig. 5 shows the two methods are in exact agreement for $M < 75$ kNm, and within 10 per cent of one another thereafter. This shows that, within the normal scatter in experimental work of this type, either method may be used to generate $M-\phi$ data, and is the first step towards the validation of the component method.

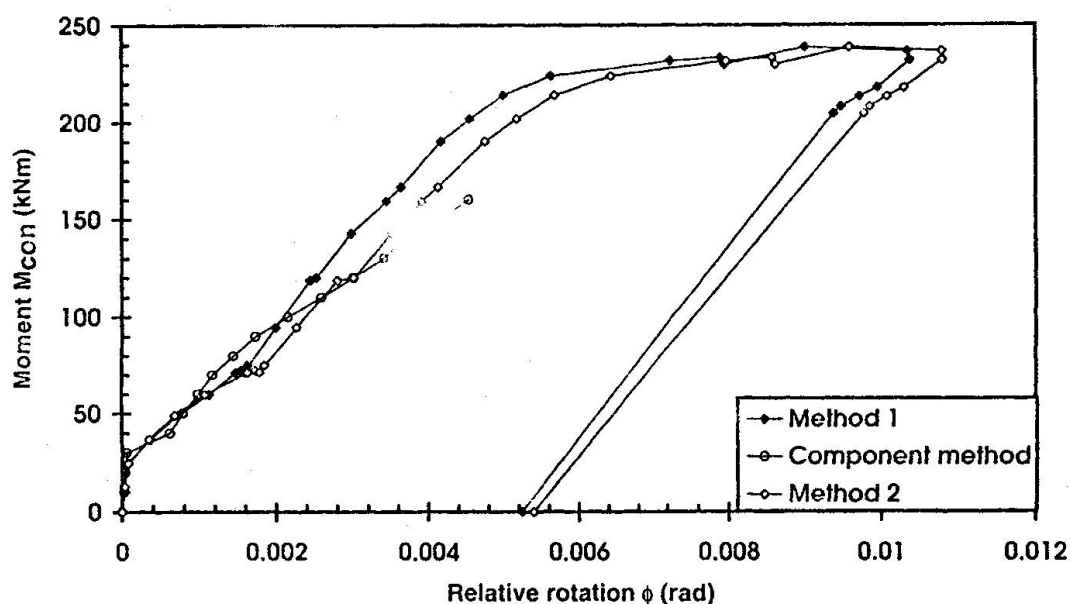


Fig. 5. Moment-rotation data obtained using three different methods.

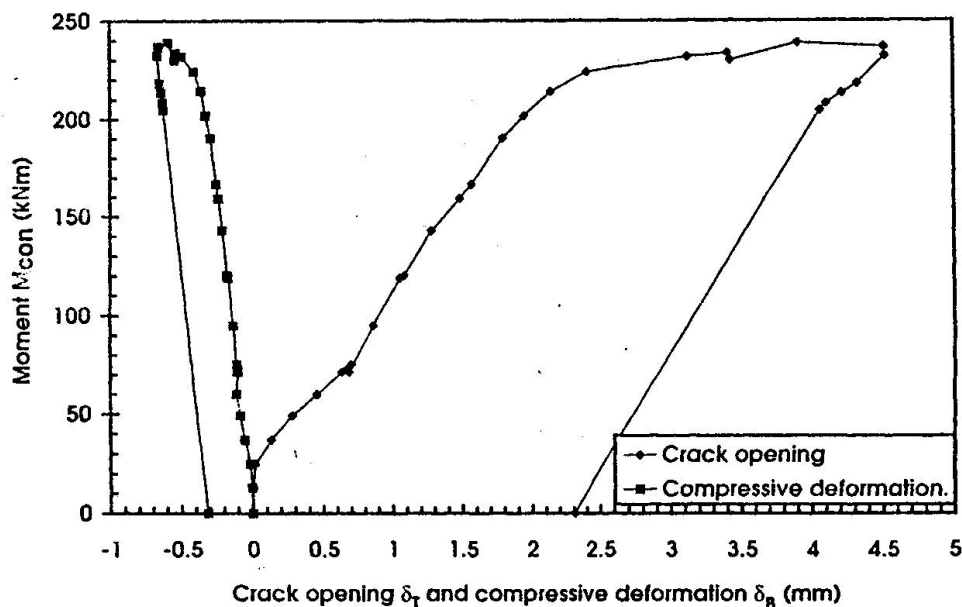


Fig. 6. Horizontal deformations vs applied moment.



Fig. 7 shows the damaged area of the joint. (The notation refers to applied load P in kN.) A circle has been drawn around the bottom right hand corner of the joint to indicate the extent of the concrete compression zone and the final position of the neutral axis, i.e. about 100 mm from the bottom of the beam. Horizontal bursting cracks are a clear indication of unconfined concrete compressive failure in the insitu concrete infill. A second horizontal crack occurs at the level of the top surface of the solid steel billet, and is possibly indicative of local stress concentrations there. The largest cracks are, as expected, at the column to joint interface. These initiated at $M = 30$ kNm, which coincides with the large reduction in stiffness seen in Fig. 5, and may be interpreted as the point at which the section is cracked flexurally.

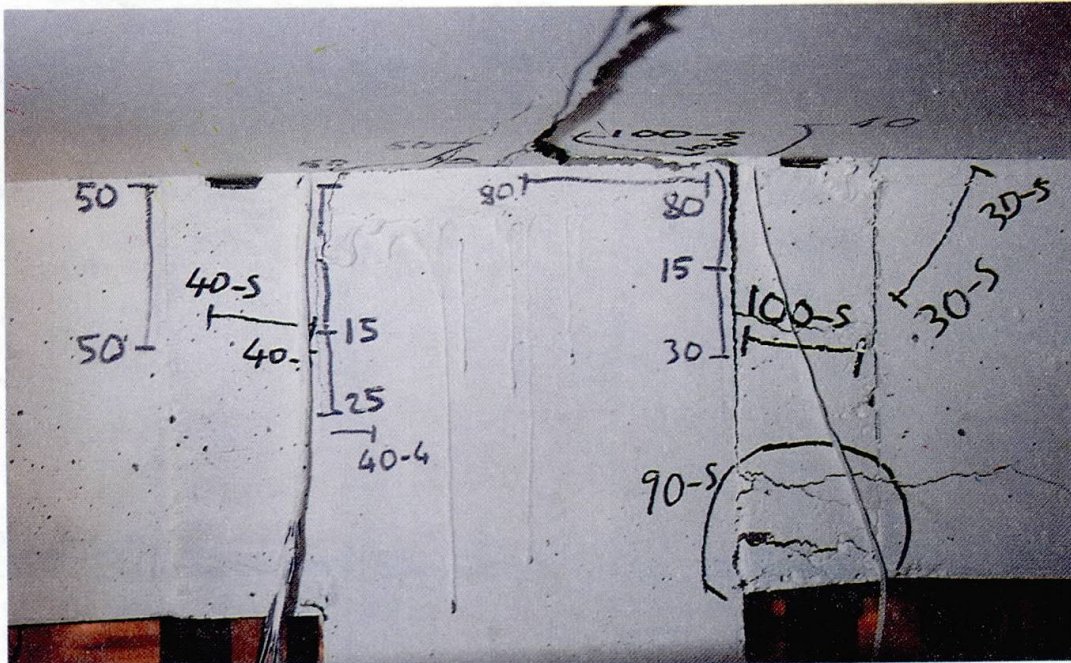


Fig. 7. Crack patterns in the vicinity of the connections in the full scale test.

3. Isolated Joint Tests

The compression zone in the bottom of the beam can be simplified as a pair of precast concrete blocks of say 100 x 100 mm cross section, one representing the beam and the other the column, joined together using a narrow strip of infill concrete of the same cross section and thickness 't' to represent the insitu infill. The shapes of the specimens are shown in Fig. 8, with the infill concrete shaded. The top of the floor slab is represented by a single reinforced concrete joint, containing 2 no. T25 bars subjected to flexural tension. The design and testing methods are described in references 4 and 5. Data for δ_T are being presented in reference 5 to enable a direct measurement of tie force vs crack width to be made.

δ_u is a function of three parameters; i) the applied stress σ ; ii) the 'effective' Young's modulus E_{cc} of the concrete; and iii) the interface deformability λ of the precast-insitu joint interface. The expression in Fig. 8 gives E_{cc} in terms of the Young's modulus for the precast and insitu concretes, E_{cp} and E_{ci} , respectively (determined experimentally from the solid specimens) and the number n of interfaces each of deformability λ . The term 'x' is the distance over which E_{cc} was determined (200 mm). Fig. 8 shows that if $E_{cp} = E_{ci}$, i.e. both concretes are the same, then $E_{cc}/E_{cp} = 1$. The fact that it is not so is indicated by the reduction attributed to the effect of t/x .

$(E_{cp}/E_{ci} - 1)$. A second reduction in E_{cc} is attributed to the joint(s) interface deformability, i.e. $n\lambda E_{cp}/x\sigma$. The small variation in E_{cc}/E_{cp} with infill thickness t may be conservatively ignored with the result that $E_{cc}/E_{cp} = 0.5$.

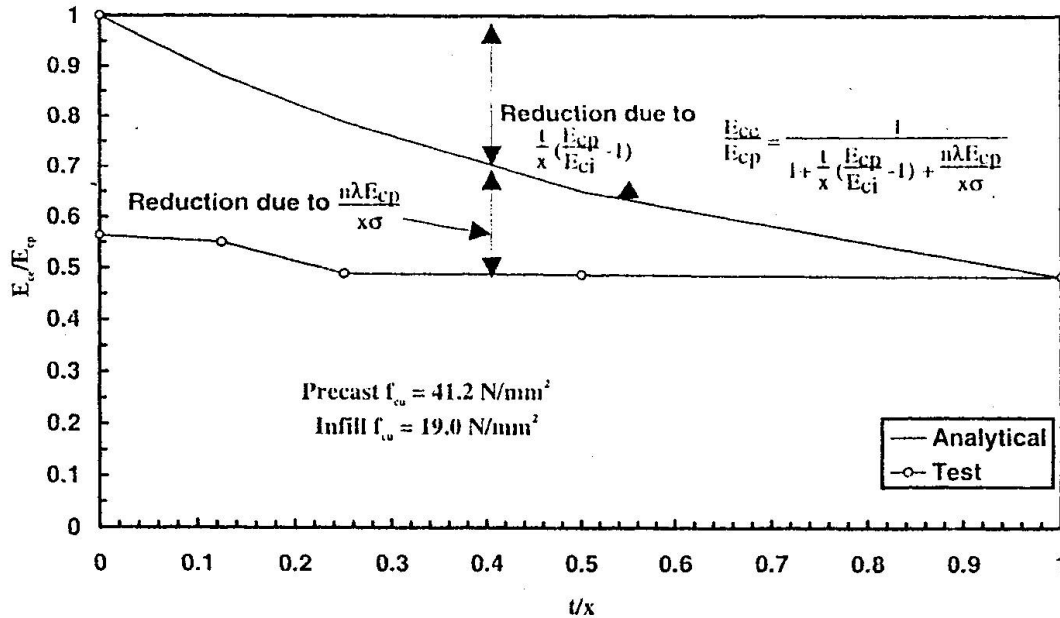


Fig. 8. Effective Young's modulus data in isolated compression tests.

Fig. 9 shows the variation in λ with applied axial stress σ for the specimens shown in Fig. 8. Although the deformability of the 'dry' joint, i.e. two precast pieces with no intermediate medium, is much greater than the 'cast' joints, it is the latter which is of interest to us. A mean constant value for $\lambda/\sigma = 0.003$ mm per N/mm^2 may be used without loss in accuracy.

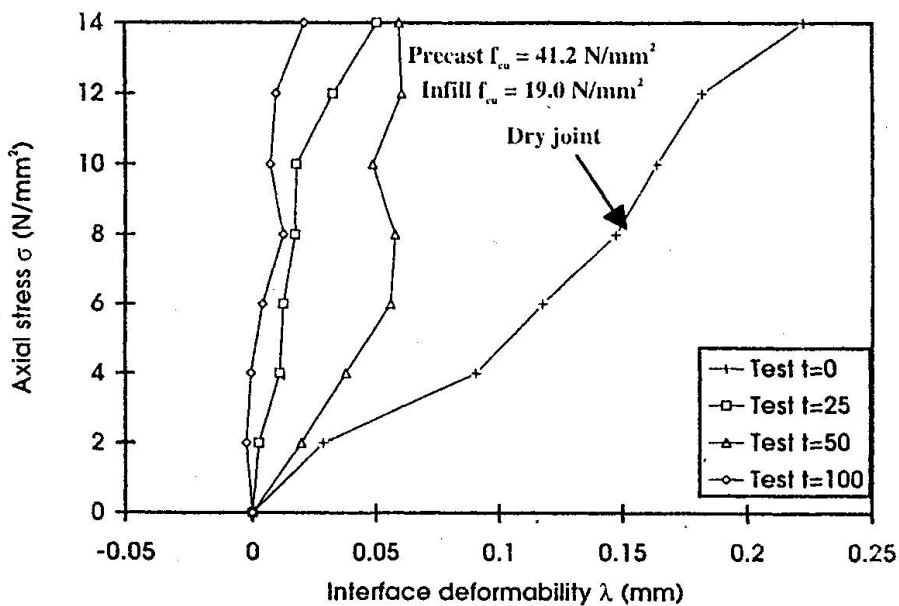


Fig. 9. Variation of joint interface deformability per interface with applied axial stress in isolated compression tests.



4. Comparison of $M-\phi$ Derived from Full Scale Tests and The Component Method.

$M-\phi$ data is derived from the component method as follows:

1. Using the flexurally uncracked section properties Z_u of the beam and floor slab (neglecting the welded plate connector), the compressive flexural stress σ in the beam is determined for a given bending moment M , i.e. $\sigma = M/Z_u$.
2. The compressive strain in the beam $\epsilon = \sigma/E_{cc}$, where E_{cc} is given in Figs. 8 and 9. Compressive deformation δ_b is determined over a gauge length of 180 mm.
3. The tie force in the top steel is equated to the total compression force in the beam. δ_r being determined directly from the aforementioned crack width test data.
4. Rotation $\phi = (\delta_b + \delta_r) / 500$.
5. Repeat steps 1 to 4 using the flexurally cracked section properties where the flexural tensile stress in the concrete exceeded the limiting value. This point coincided with the commencement of the first crack in the full scale test, i.e. at $M = 30$ kNm.

The results of this exercise are also shown in Fig. 5. The agreement with the full scale results varies between +15 and -20 per cent of the moment. However, the maximum moment achieved is only 160 kNm, i.e. two-thirds of the full scale test result, and the maximum rotation is 4.4 mrad, less than half of that achieved in the full scale test. The post-cracking stiffness of the connection in the full scale test is 38.5 kNm/mrad, whereas in the component method it is approximately 33.0 kNm/mrad.

5. Discussion

In making comparisons between the $M-\phi$ results obtained from the different methods there are a number of important features in the behaviour of the full scale test worthy of further discussion. These points are discussed in the context of gaining confidence in using the component method, and to qualify some of the (inevitable) assumptions (in italics) made.

In the full scale test a transverse flexural crack was first observed at an applied bending moment of 30 kNm (Fig. 7). This crack appeared at the column face and spread to the outer edge of the hollow cored slab. The crack widths at this point were 0.019 and 0.017 mm on either side of the column. Apart from one or two minor deviations in the results (see Fig. 5) the behaviour was generally anticipated with non-linear behaviour commencing at about 80 per cent of the ultimate moment, i.e. 190 kNm. Signs of compressive concrete failure in the bottom of the beam were evident.

Strains were also measured in the T25 tie bars in the full scale test. Because the bars were continuous through the column and the loading was symmetrical their anchorage was assured at the column face. After the concrete in the tension zone failed to take any more tensile force, these were then taken by the tie bars and this gave a rise in the steel strains. At the ultimate moment two of the strain gauges recorded strains of 7000 $\mu\epsilon$ and 5400 $\mu\epsilon$, indicating significant yielding of the bars.

In generating the $M-\phi$ data using the component method it is assumed that the strains are transferred to the steel tie bars in the isolated joint test in the same manner as in the full scale tests, even though the presence of the hollow core slabs will have an influence of this.



Compressive deformations δ_b (Fig. 6) were measured over a distance of 180 mm, i.e. 100 mm joint plus 40 mm precast beam and column. The maximum concrete strain calculated from these values is 0.0037, and being greater than 0.0035 ultimate strain at which concrete is normally assumed to fail explains the onset of failure at $M = 240$ kNm. It is important to note that the compressive concrete strain obtained from the strain gauges in the beams near to the joint zone at failure was 0.00347. The maximum moment achieved by the component method was 160 kNm, and the limiting rotation was 4.4 mrad. The failure was due to concrete crushing failure in the isolated compression tests (Fig. 8).

In the isolated tests it is impossible for strains to exceed the uniaxial limit and therefore no redistribution of stress is possible in the component method.

A good agreement was obtained between the rotations derived from Methods 1 and 2. At no point do the rotations differ by more than 0.4 mrad. Horizontal deformations at the top of the beam were in linear registration with δ_r and δ_b , showing that the beam and slab were rotating as a rigid block. These data also showed that the neutral axis for the flexurally cracked section was near to the level of the welded plate connector.

In using the component method it may be assumed that plane sections remain plane, and that full horizontal interface shear interaction between the beam and slabs is possible. It is not necessary to include for the effects of the welded joint between the steel billet and narrow plate as this point coincides with the neutral axis.

6. Conclusions

M- ϕ joint data were obtained from full scale precast concrete beam - column connection tests and compared with similar data generated using the component method. A two stage approach was used to validate the component method for this particular type of precast concrete connection:

- Stage 1. True M- ϕ data were obtained from vertical beam deflections measured within 300 mm of the face of the column. These values were within 10 per cent of those obtained by summing extreme fibre horizontal deformations.
- Stage 2. M- ϕ data were generated by summing horizontal deformations obtained from isolated, small scale compression and tension joint tests.

In comparing the results obtained from the full scale tests and the component method, it is noted that both concrete and tie steel uni-axial yield strains are exceeded in the former, whereas this is not possible in the isolated tests. For this reason the full scale ultimate test moment of 240 kNm and rotation capacity of 11 mrad are not achieved; the values being 160 kNm and 4.4 mrad, respectively. This is because no redistribution of stress is possible in isolated tests, and cracking is affected by the presence of floor slabs in the full scale tests. However, the points where the stiffness of the full scale connection changes, i.e. after the first flexural crack at 30 kNm moment, and the magnitude of the stiffness are both faithfully reproduced in the component method.

In conclusion it is such that, within the limitations described the component method provides a reasonable tool to generate M- ϕ data, and needs to be developed further.



References

- 1 Elliott, K. S., Davies, G. and Mahdi, A. A. Semi-rigid joint behaviour on columns in precast concrete buildings, COST C1 Proceedings of the 1st Workshop, Semi-rigid Behaviour of Civil Engineering Structural Connections, E.N.S.A.I.S., Strasborg, Oct. 1992, p 282 - 295.
- 2 Mahdi, A. A. Moment rotation effects on the stability of columns in precast concrete structures, PhD thesis, University of Nottingham, 1992.
- 3 Briquet, C., Guisse, S., Jaspard, J. P., Lognard, B. and Maquoi, R. Research activities under COST C1 at the Department MSM of the University of Liege, COST C1 Proceedings of the 2nd Workshop, Semi-rigid Behaviour of Civil Engineering Structural Connections, Prague, Oct. 1994, p 75 - 88.
- 4 Elliott, K. S., Davies, G. and Görgün, H. The determination of moment-rotation in semi-rigid precast concrete connections using the component method, as ref 3, p 31 - 41.
- 5 Görgün, H. Semi-rigid behaviour of connections in precast concrete structures, Dept. of Civil Engineering Report No. SR 96-001, University of Nottingham, Feb. 1996, 344 pp.

Acknowledgement

The authors wish to thank the technicians Michael Bettison, Charles Lambert, Bal Loyla, Geoff Mitchell, Melvyn Ridal and Brian Whitehead, of the Civil Engineering Laboratory at the University of Nottingham for their careful and skilled work, and to EPSRC and the Turkish Government for financial assistance.

PREDICTION OF THE FLEXURAL RESISTANCE OF BOLTED CONNECTIONS WITH ANGLES

C. Faella, V. Piluso, G. Rizzano

Department of Civil Engineering, University of Salerno, Italy

Summary

A new procedure for evaluating the flexural resistance of top and seat angle connections including web angles is presented in this paper. The main feature of the proposed procedure is its ability to account for all joint components, without any preliminary assumption concerning the failure mode. Therefore, it can be well inserted within the framework of Annex J of Eurocode 3 which, up-to-now, do not include this very common beam-to-column joint typology. The reliability of the proposed procedure is confirmed by a wide comparison with available experimental data.

1. Introduction

The procedures for evaluating the rotational behaviour of beam-to-column joints have been recently codified in Eurocode 3 with its Annex J [1], where the component method is developed with reference to the most common joint typologies: welded connections, bolted end plate connections and top and seat angle connections. The case of connections including web angles is, up-to-now, not included in Annex J, perhaps due to the additional difficulties arising with this connection typology as soon as all joint components are accounted for. In fact, even though simplified methods have been already developed for evaluating the rotational behaviour of connections with angles [2,3,4], these models refer to the behaviour of the connection only rather than to the joint as a whole, including the significant influence of the column components. In addition, the influence of some connection components is neglected. The case of bolted connections with angles becomes even more complex than the case of bolted end plate connections as soon as the interaction with the column components is accounted for.

The aim of this paper is to propose a comprehensive procedure to evaluate the flexural resistance of bolted connections with angles. The innovative feature of the proposed procedure is its ability to include all joint components without any preliminary assumption regarding the failure mode. In addition, it can be well inserted within the framework of Annex J covering the corresponding gap in modern European code. Studies to extend the procedure to the prediction of the joint rotational stiffness are currently in progress aiming at the complete development of the component approach also for this very common joint typology.

2. Prediction of the flexural resistance of connections with angles

The Annex J methodology for evaluating the joint flexural resistance can be extended to the case of connections with top and seat angles including also web angles considering that the contribution of web angles to the overall joint resistance can be determined through a procedure similar to that adopted, within the codified approach, for evaluating the flexural resistance of extended end plate connections.

The bolt rows in tension are defined as those connecting the top and web angles to the column flange. The first bolt row is the one connecting the leg of the top angle adjacent to the column flange. The second bolt row and subsequent ones are those connecting the web angles to the column flange, starting from the upper bolt row.

For each bolt row the effective design resistance has to be computed as the smallest design resistance of the basic components. The basic components involved in the evaluation of the joint flexural resistance, according to Annex J provisions, are: column web panel in shear, column web in compression, beam flange and web in compression, column flange in bending, column web in tension, beam web in tension, flange cleat in bending, bolts in tension, bolts in shear, bolts in bearing, plate in tension (top angle), plate in compression (seat angle).

The resistance of some of these components is independent of the bolt rows connected to the column flange and, therefore, they represent only a limitation to the overall design resi-

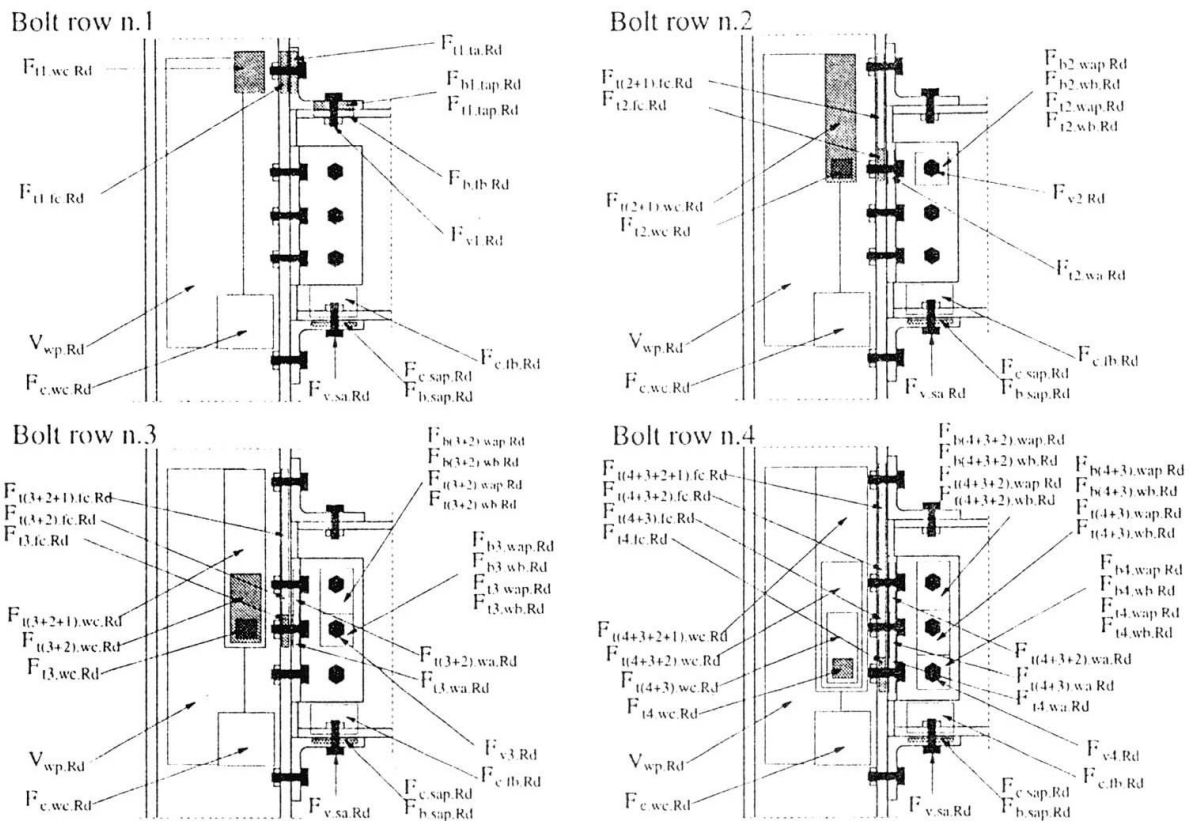


Fig. 1 - Proposed procedure for evaluating the joint flexural resistance

stance of bolt rows in tension. This is the case of the column web panel in shear $V_{wp,Rd}$, the column web in compression $F_{c,wc,Rd}$, the beam flange and web in compression $F_{c,fb,Rd}$, the bolts in shear connecting the seat angle to the beam flange $F_{v,sa,Rd}$, the bolts in bearing both with reference to the compressed beam flange $F_{b,fb,Rd}$ and to the seat angle $F_{b,sap,Rd}$, and finally the plate in compression (seat angle) $F_{c,sap,Rd}$.

On the contrary, the resistance of the remaining components is involved in the evaluation of the design tension resistance of the individual bolt rows considered both as a single bolt row and as belonging to a bolt group. This is the case of the column flange in bending (including bolts in tension) $F_{ti,fc,Rd}$ (being i the bolt row index), the column web in tension $F_{ti,wc,Rd}$, the beam web in tension $F_{ti,wb,Rd}$, the top angle in bending (including bolts in tension) $F_{t1,ta,Rd}$, the web angle in bending (including bolts in tension) $F_{ti,wa,Rd}$, the bolts in shear connecting the top angle $F_{v1,Rd}$ and the web angle $F_{vi,Rd}$ with the column flange, the bolts in bearing (with reference to the beam tension flange $F_{b,fb,Rd}$, to the top angle plate $F_{b,tap,Rd}$ and to the web angle plate $F_{bi,wap,Rd}$) and, finally, the plate in tension (top angle) $F_{t,tap,Rd}$.

Starting from the first bolt row, the proposed procedure evaluates the design tension resistance $F_{ti,Rd}$ of each bolt row as the minimum values of the resistance of its basic component (Fig.1) considering also the limitations, due to the components independent of the bolt rows, to the resistance of any bolt group constituted by the i -th bolt row and one or more bolt rows. The contribution of each bolt row to the design moment resistance of the joint is obtained multiplying $F_{ti,Rd}$ with the distance h_i between the i -th bolt row and the centre of compression which is located at mid-thickness of the seat angle adjacent to the beam flange.

The numerical procedure for evaluating the joint resistance is described, step by step, in the Appendix given at the end of this paper.

The strength of the joint components, excluding the resistance of the web angles in bending ($F_{ti,wa,Rd}$ which is analysed in the next section) and the top angle in bending ($F_{t1,ta,Rd}$ which is discussed in the section 4) are determined according the Annex J. In addition, exception is made with reference to the column web panel in shear and column web in compression whose design resistance is evaluated according to the suggestions given by the authors in previous works [5,6].

3. Design resistance of web angle in bending

The contribution of the web angles can be computed according to the model developed by Chen et al. [2,3,4]. This model is based on the following assumptions: a) the collapse mechanism of the web angle involves all its height; b) the Tresca's yield criterion combined with the Drucker shear-moment interaction is considered.

Therefore, the plastic shear force distribution V_{py} along the height of the web angle L_{wa} can be obtained by solving the following fourth-order equation:

$$\left(\frac{V_{py}}{V_{po}}\right)^4 + \frac{g_y}{t_{wa}} \frac{V_{py}}{V_{po}} = 1 \quad (1)$$

where g_y represents the distance between the two plastic hinges, developed in the web angle

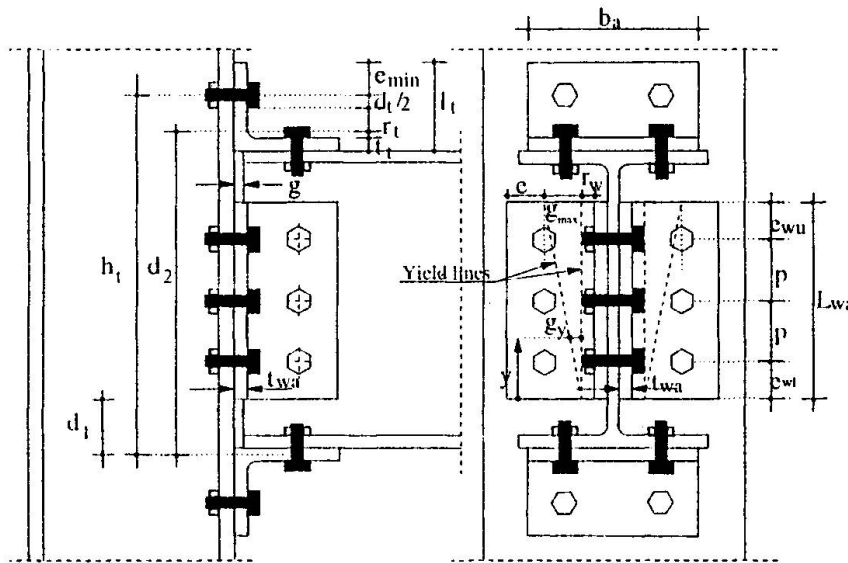


Fig. 2 - Joint geometrical parameters

leg attached to the column flange, measured at the distance y from the lower edge of the web angle and t_{wa} is the web angle tickness (Fig.2).

The solution of eq.(1) can be obtained through a numerical procedure. Therefore, in order to simplify the procedure, Chen et al. propose to assume a linear distribution of the plastic shear, as shown in Fig.3, and to locate the overall plastic shear V_{pa} of the web angle in the corresponding barycentre. Therefore, the contribution to the flexural resi-

stance due to double web angles is given by:

$$M_{j,Rd}^{(dwa)} = 2 V_{pa} d_4 \quad (2)$$

where d_4 is the distance between the point of application of V_{pa} and the centre of compression.

An alternative method, which leads to a closed form solution, can be proposed starting from an approximate moment-shear interaction based on the assumption that the external fibres withstand the bending moment, while the internal ones are subjected to shear stress only. In this case, the application of the Hencky's yield criterion leads to the following relationship:

$$\left(\frac{V_{py}}{V_{po}}\right)^2 + \frac{2}{\sqrt{3}} \frac{g_y}{t_{wa}} \left(\frac{V_{py}}{V_{po}}\right) = 1 \quad (3)$$

which has the positive solution:

$$\frac{V_{py}}{V_{po}} = \frac{1}{\sqrt{3}} \left\{ \left[\left(\alpha \frac{y}{L_{wa}} \right)^2 + 3 \right]^{1/2} - \alpha \frac{y}{L_{wa}} \right\} \quad (4)$$

where $\alpha = g_{max}/t_{wa}$ (Fig.2).



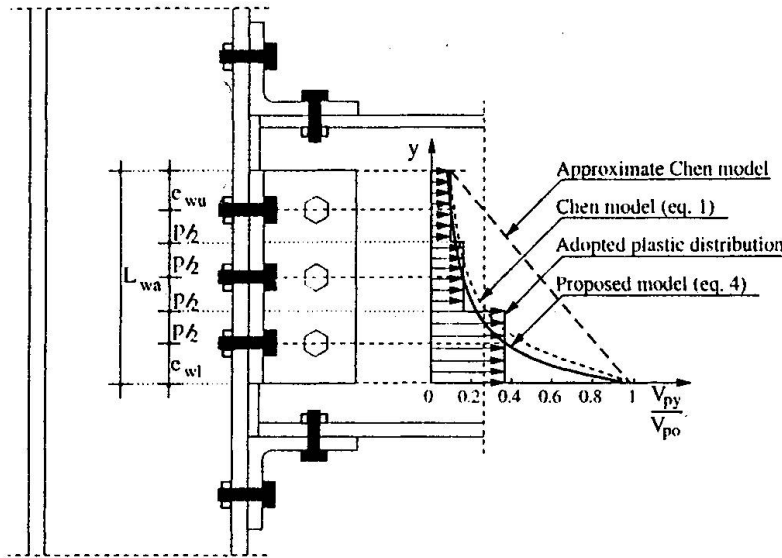
In this case, the overall plastic shear force due to the web angle V_{pa} can be obtained by integrating V_{py} over the entire height L_{wa} of the web angle:

$$V_{pa} = \left[-\frac{\sqrt{3} \ln 3}{4 \alpha} + \frac{\sqrt{3} \ln [\sqrt{\alpha^2+3} + \alpha]}{2 \alpha} + \frac{\sqrt{3} \sqrt{\alpha^2+3}}{6} - \frac{\sqrt{3} \alpha}{6} \right] L_{wa} V_{po} \quad (5)$$

In addition the distance between the overall plastic shear force, due to the web angle, and its lower edge is given by:

$$d_p = \frac{\int_0^{L_{wa}} V_{py} y dy}{\int_0^{L_{wa}} V_{py} dy} = \frac{4 L_{wa} [(\alpha^2 + 3)^{1.5} - \alpha^3 - 3 \sqrt{3}]}{3 \alpha [2 [3 \ln(\sqrt{\alpha^2 + 3} + \alpha) + \alpha(\sqrt{\alpha^2 + 3} - \alpha)] - \ln 27]} \quad (6)$$

In order to predict the web angle design resistance through a procedure based on the



a procedure based on the T-stub model adopted by Annex J, an approximate distribution of the plastic shear forces (Fig.3) can be considered. To this scope, the effective length l_{eff} of each bolt row can be defined as suggested in Table 1. According to the above distribution, the contribution of each bolt row is computed as $l_{eff} V_{py,i}$ (where $V_{py,i}$ is given by equation (4) considering the location y_i of the i -th bolt row). Furthermore, with reference to an equivalent T-stub failing according to the flange complete yielding mode [1], the above resi-

Fig. 3 - Plastic shear of the web angle

stance of the single bolt row corresponds to assume that the resistance of a couple of web angles ($2 V_{py,i} l_{eff}$) is equivalent, for each bolt row, to that of a T-stub $4 M_{pl,Rd}/m'_i$ with the parameter m'_i given by:

$$m'_i = \frac{3}{2} \frac{t_{wa}}{\left[\left(\alpha \frac{y_i}{L_{wa}} \right)^2 + 3 \right]^{1/2} - \alpha \frac{y_i}{L_{wa}}} \quad (7)$$

Therefore, within the framework of Annex J approach, the design resistance of the single bolt row of double web angles $F_{t,wa,Rd}$ can be computed as the smallest value among three possible failure modes:

Mode 1: complete yielding of angle legs

$$F_{t,wa,Rd} = \frac{4 M_{pl,Rd}}{m'_i} \quad (8)$$

where $M_{pl,Rd}$ is the plastic moment of the web angle plate with the effective length given in Table 1 and m' defined according to equation (7).

Mode 2: bolt failure with angle leg yielding

Tab. 1 - Effective length for web angles

	Bolt row considered individually		Bolt row considered as part of a bolt-group
	circular pattern l_{eff}	other patterns l_{eff}	
Bolt row adjacent to the upper edge of the web angle	$2 \pi m$	$4 m + 1.25 e$	$0.5 p + e_{ua}$
inner bolt row	$2 \pi m$	$4 m + 1.25 e$	p
Bolt row adjacent to the lower edge of the web angle	$2 \pi m$	$4 m + 1.25 e$	$0.5 p + e_{ul}$

$$F_{T2,wa,Rd} = \frac{M_{pl,Rd} + n \sum B_{T,Rd}}{m + n} \quad (9)$$

where $B_{T,Rd}$ is the design tension resistance of a bolt-plate assembly, m is the distance between the bolt axis and the plastic hinge, n is the distance between the bolt axis and the prying force. Both m and n are defined according to Annex J [1].

Mode 3: bolt failure

$$F_{T3,wa,Rd} = \sum B_{T,Rd} \quad (10)$$

Obviously, in the case of single web angle connections the above contributions have to be halved.

4. Contribution of the top angle in bending to the overall joint resistance

According to Annex J, the top angle can be modelled as an equivalent T-stub characterized by $l_{eff} = 0.5b_a$, where b_a is the length of the cleat, and m is the following geometrical parameter:

$$m = l_t - e_{min} - t_t - 0.8 r_t \quad \text{for } g \leq t_t \quad \text{and} \quad m = l_t - e_{min} - l_t/2 \quad \text{for } g > t_t \quad (11)$$

where g , l_t , e_{min} , t_t , r_t are given in Fig.2.

Therefore, the contribution of the top angle to the joint flexural resistance can be obtained as:

$$M_{j,Rd}^{(ta)} = F_{T,ta,Rd} h_t \quad (12)$$

provided that the weakest component for the first bolt row is represented by the top angle in bending. $F_{T,ta,Rd}$ is the design resistance of the top angle computed through equations (8-10) with the m parameter given by equation (11), assuming in this case $m_i' = m$, and h_t is the distance between the bolt row axis of the top angle leg attached to the column flange and the centre of compression.

A different model for evaluating the flexural resistance of top and seat angle connections has been proposed by Chen et al. [2,3,4]. This model is based on the complete yielding of the cleat. The contribution of the top and seat angles to the connection flexural resistance is given by:

$$M_{j,Rd}^{(ta)} = M_{os} + M_{pt} + V_{pt} d_2 \quad (13)$$

where M_{os} is the plastic moment of the seat angle leg adjacent to the beam flange, M_{pt} and V_{pt} are the combined plastic moment and shear force of the top angle leg adjacent to the column flange and d_2 is the distance shown in Fig.2.

The main differences between the Chen model and the Annex J model are due to the fact that the former considers also moment-shear plastic interaction. In addition, with reference to the complete yielding failure mode, different definitions of the distance between the plastic hinges are used. In fact, according to Chen model, the above distance is given by:

$$m_c = l_t - e_{min} - d_t/2 - 1.5 t_t - r_t \quad (14)$$

(where d_t is the bolt head diameter), while it is defined through the parameter m in Annex J (11). It is evident that m and m_c provide the upper and the lower bound, respectively, for the distance between the plastic hinges in complete yielding failure mode.



In order to evaluate the reliability of the models previously described, the available experimental results concerning top and seat angles with single/double web angle connections have been analysed. In particular, 29 experimental results collected in the SCDB data Bank [7] and in the Sericon data bank [8] have been considered. A first group of experimental tests, due to Azizinamini et al. [9,10], provides the behaviour of top and seat angles with double web angles connections (T-S-DW), while a second group of tests, due to Schleich et al. [8], refers to top and seat angles with single web angle connections (T-S-SW).

The experimental flexural resistance of the joints has been conventionally assumed equal to the experimental value of the $M - \phi$ curve corresponding to a secant stiffness equal to $K_{\phi,s} = K_{\phi,i}/3$, where $K_{\phi,i}$ is the initial rotational stiffness (the slope of the elastic reloading branch of the $M - \phi$ curve, when it is not specified by the test authors). In addition, in order to define for the moment-rotation curve predicted according to the Chen power model [2,3,4] a knee (i.e. a design value) compatible with Annex J, the same procedure has been applied considering the curve evaluated on the basis of the three parameters K_{ϕ} , M_u and n and by adopting for the shape factor n the values suggested in [11].

The influence of the m and m_c parameters is evidenced in Table 2 and Figures 4a and 4b by the comparison between the results obtained with the Chen model and those obtained with the procedure previously described and by assuming an m definition compatible with Annex J (11). Furthermore, in Table 3, the main statistical parameters of the ratio $M_{j,Rd}/M_{exp}$ between the predicted joint resistance $M_{j,Rd}$ and the experimental one M_{exp} are shown, both with reference to the single groups of tests and with reference to all the available experimental results ($M_{j,Rd}$ defines the knee of the $M - \phi$ curve).

It is important to underline that generally the Chen model provides a slight overestimation of the design flexural resistance while the use of an m value compatible with Annex J gives rise to an underestimation of the resistance.

The role of all joint components can be evidenced by comparing the results obtained for the different groups of tests. In fact, the tests of Schleich et al. are characterized by the use of the same angle both for the beam web-to-column flange connection and for the beam flange-to-column flange connection. In addition, the angle thickness is very significant, as the ratio between the column flange thickness and the angle thickness is close to 1.0 (Table 2). On the contrary, the tests of Azizinamini et al. have a small angle thickness compared to

Tab. 2 - Influence of m parameter

N. test	CODE	AUTHORS	Joint type	M_{exp} (kNm)	Chen model			Model m as (11)		$\frac{t_f}{t_w}$	$\frac{t_c}{t_w}$
					M_u (kNm)	$M_{j,Rd}$ (kNm)	$\frac{M_{j,Rd}}{M_{exp}}$	M_{Rd} (kNm)	$\frac{M_{j,Rd}}{M_{exp}}$		
1	8S1	Azizinamini et al.	T-S-DW	30.39	38.55	37.83	1.24	17.79	0.59	2.56	2.05
2	8S2	Azizinamini et al.	T-S-DW	38.43	50.73	47.78	1.24	22.54	0.59	2.56	1.71
3	8S3	Azizinamini et al.	T-S-DW	39.12	47.15	46.02	1.18	20.78	0.53	2.56	2.05
4	8S4	Azizinamini et al.	T-S-DW	20.65	21.15	21.15	1.02	13.39	0.65	2.56	1.71
5	8S5	Azizinamini et al.	T-S-DW	33.49	43.12	42.73	1.28	21.82	0.65	2.56	1.71
6	8S6	Azizinamini et al.	T-S-DW	25.13	27.24	27.16	1.08	15.29	0.61	2.56	2.05
7	8S7	Azizinamini et al.	T-S-DW	40.50	35.56	35.30	0.87	18.59	0.46	2.56	1.71
8	8S8	Azizinamini et al.	T-S-DW	36.36	40.86	39.41	1.08	17.31	0.48	2.56	2.05
9	8S9	Azizinamini et al.	T-S-DW	35.28	52.80	45.88	1.30	21.93	0.62	2.56	1.71
10	8S10	Azizinamini et al.	T-S-DW	44.21	76.64	39.19	0.89	35.43	0.80	2.56	1.28
11	14S1	Azizinamini et al.	T-S-DW	63.20	81.78	78.15	1.24	41.47	0.66	3.60	2.40
12	14S2	Azizinamini et al.	T-S-DW	87.45	168.17	153.83	1.76	80.05	0.92	3.60	1.80
13	14S3	Azizinamini et al.	T-S-DW	65.31	71.15	66.53	1.02	35.84	0.55	3.60	2.40
14	14S4	Azizinamini et al.	T-S-DW	77.22	103.80	98.85	1.28	59.19	0.77	2.40	2.40
15	14S5	Azizinamini et al.	T-S-DW	89.44	84.53	78.07	0.87	40.34	0.45	3.60	2.40
16	14S6	Azizinamini et al.	T-S-DW	89.30	133.01	68.01	0.76	60.23	0.67	3.60	1.80
17	14S8	Azizinamini et al.	T-S-DW	131.40	178.32	91.18	0.69	88.31	0.67	3.60	1.44
18	14S9	Azizinamini et al.	T-S-DW	99.17	133.01	68.01	0.69	60.23	0.61	3.60	1.80
19	103001	Schleich et al.	T-S-SW	37.91	70.44	61.63	1.63	25.63	0.68	1.41	1.41
20	103002	Schleich et al.	T-S-SW	47.92	82.88	42.38	0.88	29.96	0.63	1.11	1.11
21	103003	Schleich et al.	T-S-SW	43.99	107.27	54.85	1.25	36.96	0.84	1.41	1.41
22	103004	Schleich et al.	T-S-SW	60.01	123.02	62.91	1.05	43.94	0.73	1.11	1.11
23	103005	Schleich et al.	T-S-SW	77.33	144.08	73.68	0.95	46.22	0.60	1.41	1.41
24	103045	Schleich et al.	T-S-SW	44.59	70.44	61.63	1.38	25.63	0.57	1.41	1.41
25	103046	Schleich et al.	T-S-SW	42.97	82.88	42.38	0.99	29.96	0.70	1.11	1.11
26	103047	Schleich et al.	T-S-SW	60.27	107.27	54.85	0.91	36.96	0.61	1.41	1.41
27	103048	Schleich et al.	T-S-SW	36.00	123.02	62.91	1.75	43.94	1.22	1.11	1.11
28	103049	Schleich et al.	T-S-SW	49.85	144.08	73.68	1.48	46.22	0.93	1.41	1.41
29	103050	Schleich et al.	T-S-SW	62.27	164.91	84.33	1.35	55.10	0.88	1.11	1.11



Tab. 3 - Statistical results of the comparison

	Chen et al. model		Model with m as (11)	
	Average	Standard deviation	Average	Standard deviation
Azizinamini et al.	1.08	0.27	0.63	0.12
Schleich et al.	1.24	0.30	0.76	0.19
Total	1.14	0.29	0.68	0.16

that of the column flange. In particular, with reference to the web angle, the above mentioned ratio ranges from 2.40 to 3.60.

As a consequence of the above geometrical features, the weakest component is given by the angles (both top $t.ta$ and web $t.wa$ angles) in the specimens tested by Azizinamini et al. On the contrary, a significant interaction between the column flange ($t.fc$) and web angles occurs in the tests of Schleich et al.

The proposed method can be improved provided that, with reference to the case of complete yielding, a more appropriate value m^* of the distance between the angle plastic hinges is defined considering that the values proposed by Annex J and Chen represent the boundary values of the variability range. The following definition of m^* can be adopted:

$$m^* = m - \psi (d_t/2 + t_t/2 + 0.2 r_t) \tag{15}$$

where ψ is a coefficient ranging from 0 to 1. Obviously, the 0 value corresponds to the Annex J definition while the value 1.0 corresponds to the Chen model.

The m^* parameter is used both with reference to the top angle and with reference to the web angle. In the latter case m^* defines the location of the yield line at the level of the upper bolt row of the web angle (Fig.2).

The coefficient ψ can be related to the ratio between the flexural stiffness of the angle leg attached to the column flange and the axial stiffness of the bolts connecting the angles to the column. On the basis of the experimental tests of Azizinamini et al., which are characterized by the collapse of top and web angles, the following relationship has been found:

Tab. 4 - Reliability of the proposed method including the coefficient ψ

N. test	CODE	AUTHORS	M_{exp} (kNm)	Proposed method									
				Collapse mode				ψ		$M_{jRd}^{(m)}$ (kNm)	$M_{jRd}^{(m^*)}$ (kNm)	M_{Rd} (kNm)	$\frac{M_{Rd}}{M_{exp}}$
				row 1	row 2	row 3	row 4	top ang.	web ang.				
1	8S1	Azizinamini et al.	30.39	t.ta	t.wa	t.wa	-	0.86	1.00	25.63	9.05	34.68	1.14
2	8S2	Azizinamini et al.	38.43	t.ta	t.wa	t.wa	-	0.63	1.00	30.36	8.40	38.76	1.01
3	8S3	Azizinamini et al.	39.12	t.ta	t.wa	t.wa	-	0.86	1.00	34.17	7.54	41.71	1.07
4	8S4	Azizinamini et al.	20.65	t.ta	t.wa	t.wa	-	1.00	1.00	8.84	10.72	19.56	0.95
5	8S5	Azizinamini et al.	33.49	t.ta	t.wa	t.wa	-	0.83	1.00	28.54	7.64	36.18	1.08
6	8S6	Azizinamini et al.	25.13	t.ta	t.wa	t.wa	-	1.00	1.00	15.76	10.21	25.97	1.03
7	8S7	Azizinamini et al.	40.50	t.ta	t.wa	t.wa	-	0.83	1.00	21.41	9.14	30.55	0.75
8	8S8	Azizinamini et al.	36.36	t.ta	t.wa	t.wa	-	0.94	1.00	35.19	7.90	43.09	1.19
9	8S9	Azizinamini et al.	35.28	t.ta	t.wa	t.wa	-	0.73	1.00	38.51	7.53	46.04	1.31
10	8S10	Azizinamini et al.	44.21	t.ta	t.wa	t.wa	-	0.25	1.00	41.91	7.39	49.30	1.12
11	14S1	Azizinamini et al.	63.20	t.ta	t.wa	t.wa	t.wa	0.83	1.00	43.87	22.47	66.34	1.05
12	14S2	Azizinamini et al.	87.45	t.ta	t.wa	t.wa	t.wa	0.42	1.00	84.11	15.41	99.52	1.14
13	14S3	Azizinamini et al.	65.31	t.ta	t.wa	t.wa	t.wa	0.83	1.00	43.87	15.33	59.20	0.91
14	14S4	Azizinamini et al.	77.22	t.ta	t.wa	t.wa	t.wa	0.83	0.95	43.87	41.17	85.04	1.10
15	14S5	Azizinamini et al.	89.44	t.ta	t.wa	t.wa	t.wa	0.91	1.00	50.95	22.32	73.27	0.82
16	14S6	Azizinamini et al.	89.30	t.ta	t.wa	t.wa	t.wa	0.53	1.00	72.17	19.93	92.10	1.03
17	14S8	Azizinamini et al.	131.40	t.ta	t.wa	t.wa	t.wa	0.00	1.00	80.20	14.15	94.35	0.72
18	14S9	Azizinamini et al.	99.17	t.ta	t.wa	t.wa	t.wa	0.53	1.00	72.17	19.93	92.10	0.93
19	103001	Schleich et al.	37.91	t.ta	t.wa	t.fc	-	0.40	0.57	27.87	-	29.83	0.79
20	130002	Schleich et al.	47.92	t.ta	t.fc	t.fc	-	0.00	0.17	27.87	-	29.96	0.63
21	103003	Schleich et al.	43.99	t.ta	t.wa	t.fc	-	0.56	0.70	48.38	-	52.15	1.19
22	103004	Schleich et al.	60.01	t.ta	t.fc	t.fc	-	0.16	0.34	43.25	-	48.26	0.80
23	103005	Schleich et al.	77.33	t.ta	t.wa	t.fc	-	0.56	0.70	64.03	-	65.73	0.85
24	103045	Schleich et al.	44.59	t.ta	t.wa	t.fc	-	0.40	0.57	27.87	-	29.83	0.67
25	103046	Schleich et al.	42.97	t.ta	t.fc	t.fc	-	0.00	0.17	27.87	-	29.96	0.70
26	103047	Schleich et al.	60.27	t.ta	t.wa	t.fc	-	0.56	0.70	48.38	-	52.15	0.87
27	103048	Schleich et al.	36.00	t.ta	t.fc	t.fc	-	0.16	0.34	43.25	-	48.26	1.34
28	103049	Schleich et al.	49.85	t.ta	t.wa	t.fc	-	0.56	0.70	64.03	-	65.73	1.32
29	103050	Schleich et al.	62.27	t.ta	t.fc	t.fc	-	0.16	0.35	57.19	-	60.59	0.97

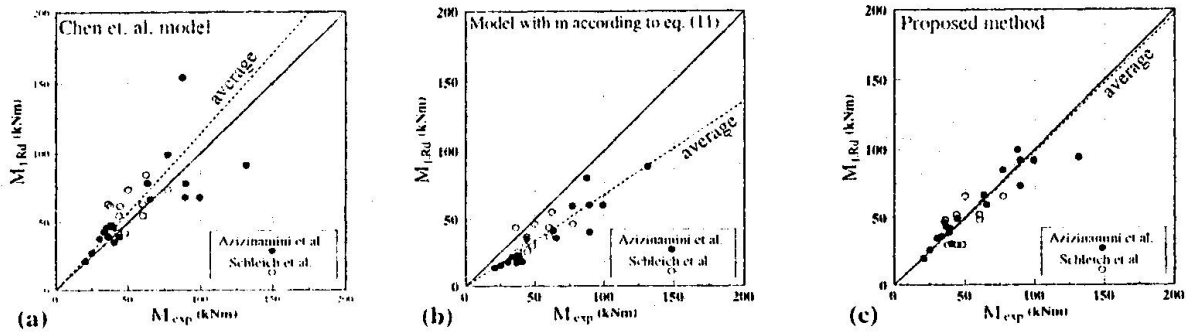


Fig.4 - Reliability of different procedures for predicting the flexural resistance

$$0 \leq \psi = 1.89 - 3.22 \left(\frac{t}{d_b \sqrt{m/d_b}} \right) \leq 1 \tag{16}$$

In Tab. 4 and fig. 4c, the comparison between the predicted values of the flexural resistance $M_{j,Rd}$, evaluated with the proposed procedure including also the coefficient ψ , and the experimental ones are shown.

A good degree of accuracy can be observed, as it is evidenced by the average value and the standard deviation of $M_{j,Rd}/M_{exp}$ ratio (Tab.5). In particular, the check of the resistance of all joint components has led to a good degree of approximation also with reference to the tests of Schleich et al.

With reference to the cases in which the weakest component is represented by the top and web angles, it is useful to underline that the contribution to the joint resistance of the web angle is not negligible. In fact, this contribution ranges from 15% to 30% of the global joint resistance with an average value equal to 26% as it can be noted in table 4 where the contributions to the joint flexural resistance $M_{j,Rd}^{(ta)}$ and $M_{j,Rd}^{(wa)}$ due to the top and web angles, respectively, are given.

5. Simplified procedure for evaluating the joint design resistance

Even though the advantages of a general procedure accounting for all joint components have been clarified in the previous section, a simplified method could be adopted provided that the joint resistance is governed by angles and, in addition, the bolts of the web angles are closely spaced to assure the failure as a bolt group rather than individually. In this case, the design resistance of the web angle can be obtained as the minimum value given by equation (5) and equations (9) and (10), where $l_{eff} = L_{wa}$ has to be assumed.

Moreover, it can be observed that the resistance corresponding to the first collapse mode, given by equation (5) can be equivalently obtained by means of the T-Stub model (equation (8)) provided that the following value of the parameter m' is adopted:

$$m' = \frac{\sqrt{3} t_{wa}}{2 \left[\frac{\sqrt{3} \ln 3}{4 \alpha} + \frac{\sqrt{3} \ln [\sqrt{\alpha^2+3} + \alpha]}{2 \alpha} + \frac{\sqrt{3} \sqrt{\alpha^2+3}}{6} - \frac{\sqrt{3} \alpha}{6} \right]} \tag{17}$$

Therefore, the joint design resistance can be evaluated by means of the following relationship:

$$M_{j,Rd} = F_{t,Rd} h_t + F_{w,Rd} h_w \tag{18}$$

where $F_{t,Rd}$ is the design resistance of the top angle evaluated according to the previous section, $F_{w,Rd}$ is the design resistance of the web angle computed as the minimum value given by the equations (8) (with m' given by eq. (17)), (9) and (10). In addition, the lever arm h_w of the web angle contribution is given by d_p (equation (6)) plus the distance between the lower edge of web angles and the center of compression (d_1), when the complete yielding of flange arises, or by the distance between the middle length of the web angle and the centre of compression for collapse modes 2 and 3.

Tab. 5 - Statistical results of the comparison between the predicted and experimental resistance

	Proposed procedure (all joint components)		Simplified proposed procedure (top and web angle components)	
	Average	Standard deviation	Average	Standard deviation
Azizinamini et al.	1.02	0.15	1.05	0.17
Schleich et al.	0.92	0.25	1.31	0.37
Total	0.98	0.20	1.15	0.29

In table 5, the comparison between the predicted values and the experimental ones of the joint flexural resistance is given with reference to the main statistical parameters of the ratio $M_{j,Rd}/M_{exp}$.

A good degree of approximation of the simplified method can be mainly observed with reference to the Azizinamini et al. tests, which satisfy the basic hypotheses of the method. This degree of accuracy, as expected, is comparable with the one obtained by the Chen model. With respect to this, the proposed procedure presents further simplifications. In fact, the use of the shear-moment interaction according to eq.(3) allows to compute in closed form the overall shear force (5) and the corresponding location (6), due to the web angles. Numerical procedures are required by the Chen model. In addition, even though simplified, also this approach can be considered within the framework of Annex J. However, it should be underlined that a parametric analysis with the general method including all joint components is necessary with the aim to provide the «a priori» knowledge of the validity range of the simplified procedure.

6. Conclusion

The extension of the component method of Annex J to the case of connections with angles, including web angles, has been proposed in this paper. The reliability of the suggested procedure has been confirmed by the comparison with the available experimental tests on this connection typology. The importance to account for all joint components has been underlined considering tests from different authors, i.e. characterized by different geometrical details. In addition, a simplified procedure has been also proposed. This procedure can be applied provided that the web angles fail involving their full depth.

7. References

- [1] Eurocode 3, part 1.1: Revised Annex J: Joints in Building Frames
- [2] N. Kishi, W.F. Chen, K.G. Matsuoka, S.G. Nomachi: Moment-Rotation Relation of Top- and Seat-Angle with Double Web-Angle Connections. Proc. Workshop on Connections and the Behaviour, Strength and Design of Steel Structures, Elsevier Applied Science, London, 1987
- [3] N. Kishi, W.F. Chen, K.G. Matsuoka, S.G. Nomachi: Moment-Rotation Relation of Single-Double Web-Angle Connections. Proc. Workshop on Connections and the Behaviour, Strength and Design of Steel Structures, Elsevier Applied Science, London, 1987
- [4] N. Kishi, W.F. Chen: Moment-Rotation Relations of Semirigid Connections with Angles, Journal of Structural Engineering, ASCE, Vol.116, No. 7, July, 1990.
- [5] C. Faella, V. Piluso, G. Rizzano: Modelling of the moment-rotation curve of welded connections: proposals to improve eurocode 3 Annex J, C.T.A., Italian Conference on Steel Construction, Riva del Garda, October, 1995.
- [6] C. Faella, V. Piluso, G. Rizzano: Some proposals to improve EC3-Annex J approach for predicting the moment-rotation curve of extended end plate connections, C.T.A., Italian Conference on Steel Construction, Riva del Garda, October, 1995.
- [7] N. Kishi, W.F. Chen: Database of Steel Beam-to-Column Connections, Structural Engineering Report, No. CE-STR-86-26, School of Civil Engineering, Purdue University, 1986.
- [8] K. Weinand: SERICON - Databank on joints in building frames, Proceedings of the 1st COST C1 Workshop, Strasbourg, 28-30 October.
- [9] A. Azizinamini, J.H. Bradburn, J.B. Radziminski: Initial Stiffness of Semi-Rigid Steel Beam-to-Column Connections, Journal of Constructional Steel Research, Vol. 8, 1987.
- [10] A. Azizinamini, J.B. Radziminski: Static and Cyclic Performance of Semirigid Steel Beam-to-Column Connections, Journal of Structural Engineering, Vol.115, No.12, 1989.



- [11] J.Y.R. Liew, D.W. White, W.F. Chen: Limit State Design of Semi-Rigid Frames using Advanced Analysis: Part I: Connection Modeling and Classification, Journal of Constructional Steel Research, Vol.26, 1993.

APPENDIX

With reference to Fig.1, the proposed procedure can be performed by means of the following steps:

- a) evaluation of the design tension resistance of the first bolt row ($F_{t1,Rd}$) as the one of the weakest component:

$$F_{t1,Rd} = \min \left\{ V_{wp,Rd}/\beta, F_{c,wc,Rd}, F_{c,fb,Rd}, F_{v,sa,Rd}, F_{b,sap,Rd}, F_{c,sap,Rd}, F_{t,fc,Rd}, F_{t,wc,Rd}, F_{t,sa,Rd}, F_{v,Rd}, F_{b,sap,Rd}, F_{b,fb,Rd}, F_{t,sap,Rd} \right\} \quad (A.1)$$

where β is a coefficient accounting for the influence of the actions, at the member ends, on the shear force in the panel zone [1].

- b) computation of the design tension resistance $F_{t2,Rd}$ of the second bolt row (i.e. the upper bolt row of the web angle) through the minimum value provided by the following limitations (A.2-A.5):

$$F_{t2,Rd} = \min \left\{ V_{wp,Rd}/\beta - F_{t1,Rd}, F_{c,wc,Rd} - F_{t1,Rd}, F_{c,fb,Rd} - F_{t1,Rd}, F_{v,sa,Rd} - F_{t1,Rd}, F_{b,sap,Rd} - F_{t1,Rd}, F_{c,sap,Rd} - F_{t1,Rd} \right\} \quad (A.2)$$

which accounts for the limitations to the resultant of the first two bolt rows due to the web panel in shear, the column web in compression, the beam flange and web in compression and the seat angle (in shear, bearing and compression);

$$F_{t2,Rd} = \min \left\{ F_{t2,fc,Rd}, F_{t(1+2)fc,Rd} - F_{t1,Rd} \right\} \quad (A.3)$$

which takes into account the limitations due to the column flange in bending considering the second bolt row both individually and as constituting a bolt group with the first bolt row;

$$F_{t2,Rd} = \min \left\{ F_{t2,wc,Rd}, F_{t(1+2)wc,Rd} - F_{t1,Rd} \right\} \quad (A.4)$$

which is a limitation similar to the previous one, but with reference to the column web in tension;

$$F_{t2,Rd} = \min \left\{ F_{t2,wa,Rd}, F_{v2,Rd}, F_{b2,wap,Rd}, F_{b2,wb,Rd}, F_{t2,wap,Rd}, F_{t2,wb,Rd} \right\} \quad (A.5)$$

which considers the limitations due to the web angle in bending, the bolts in shear, the web angle plate in bearing, the web beam in bearing, the web angle plate in tension and the web beam in tension.

- c) evaluation of the design resistance of the subsequent tension bolt rows (i.e. that of the i -th bolt row $F_{ti,Rd}$) as the minimum value obtained from the following limitations (eq. A.6-A.12):

$$F_{ti,Rd} = \min \left\{ V_{wp,Rd}/\beta - \sum_{j=1}^{i-1} F_{tj,Rd}, F_{c,wc,Rd} - \sum_{j=1}^{i-1} F_{tj,Rd}, F_{c,fb,Rd} - \sum_{j=1}^{i-1} F_{tj,Rd}, F_{v,sa,Rd} - \sum_{j=1}^{i-1} F_{tj,Rd}, F_{b,sap,Rd} - \sum_{j=1}^{i-1} F_{tj,Rd}, F_{c,sap,Rd} - \sum_{j=1}^{i-1} F_{tj,Rd} \right\} \quad (A.6)$$

which is similar to limitation (2), but including all the bolt rows above the i -th one;

$$F_{ti,Rd} = \min \left\{ F_{ti,fc,Rd}, F_{t(i+(i-1)fc,Rd} - F_{t(i-1),Rd}, \dots, F_{t(i+(i-1)+\dots+1)fc,Rd} - \sum_{j=1}^{i-1} F_{tj,Rd} \right\} \quad (A.7)$$

$$F_{ti,Rd} = \min \left\{ F_{ti,wc,Rd}, F_{t(i+(i-1)wc,Rd} - F_{t(i-1),Rd}, \dots, F_{t(i+(i-1)+\dots+1)wc,Rd} - \sum_{j=1}^{i-1} F_{tj,Rd} \right\} \quad (A.8)$$

$$F_{ti,Rd} = \min \left\{ F_{ti,wa,Rd}, F_{t(i+(i-1)wa,Rd} - F_{t(i-1),Rd}, \dots, F_{t(i+(i-1)+\dots+1)wa,Rd} - \sum_{j=1}^{i-1} F_{tj,Rd} \right\} \quad (A.9)$$

$$F_{ti,Rd} = \min \left\{ F_{ti,wap,Rd}, F_{t(i+(i-1)wap,Rd} - F_{t(i-1),Rd}, \dots, F_{t(i+(i-1)+\dots+1)wap,Rd} - \sum_{j=1}^{i-1} F_{tj,Rd} \right\} \quad (A.10)$$

$$F_{ti,Rd} = \min \left\{ F_{ti,wb,Rd}, F_{t(i+(i-1)wb,Rd} - F_{t(i-1),Rd}, \dots, F_{t(i+(i-1)+\dots+1)wb,Rd} - \sum_{j=1}^{i-1} F_{tj,Rd} \right\} \quad (A.11)$$

$$F_{ti,Rd} = \min \left\{ F_{vi,Rd}, F_{bi,wap,Rd}, F_{bi,wb,Rd} \right\} \quad (A.12)$$

- d) computation of the design moment resistance $M_{j,Rd}$ of the beam-to-column joint by means of the relationship:

$$M_{j,Rd} = \sum_{i=1}^r h_i F_{ti,Rd} \quad (A.13)$$

in which h_i is the distance between the i -th bolt row and the centre of compression and r is the number of bolt rows in tension.

Moment capacity of beam-to-column minor-axis joints

Fernando GOMES
Assistant
Dep. of Civil Eng.
University of Coimbra
Portugal

Jean-Pierre JASPART
Associate Researcher
Dep. MSM
University of Liège
Belgium

René MAQUOI
Professor
Dep. MSM
University of Liège
Belgium

Summary

This paper presents a method of prediction the moment capacity of beam-to-column minor-axis joints, where the beam is directly connected to the web of an I section column, causing bending about the minor-axis of the column section. The strength is limited by the formation of plastic failure mechanisms in the column web. Several failure modes for bolted and welded connections are discussed, and a design method based on yield line theory is proposed. The method is also applicable to the design of connections between a beam and a RHS column.

1. Introduction

Fig. 1 shows some common types of beam-to-column minor-axis joints where the beam is directly connected to the column web without stiffeners. The connection can be welded or bolted using web cleats, flange cleats, flush end plates or extended end plates.

The revised Annex J [1] of the Eurocode 3 provides design rules for the evaluation of the resistance of connecting elements (end plates, cleats, bolts) but it does not cover the common case of failure due to the out-of-plane deformation of the column web.

Failure mechanisms of the column web are briefly described in this paper and it should be emphasised that the same kind of mechanisms can be observed in the case of connections between a beam and a rectangular hollow section (RHS) column, Fig. 2. These failure mechanisms are divided into two main groups: *Local* and *Global* mechanisms, described hereafter. A local failure means that the yield line pattern is localised only in the compression zone or in the tension zone, Fig. 3, while in the global failure the yield line pattern involves both compression and tension zones, Fig. 4.

The moment transmitted by the beam to the column web may be decomposed in a couple of forces F acting in the compression and tension zones. Two different loading cases are analysed:

- *Loading case 1*: the load F acts on a rigid rectangle with the dimensions $b \times c$, Fig. 5, as in the case of a welded connection where these dimensions are defined by the perimeter of the welds around the beam flange;
- *Loading case 2*: the load F is transmitted by one or more rows of bolts, as in the tension zone of the bolted connections represented in Fig. 6 and 8.

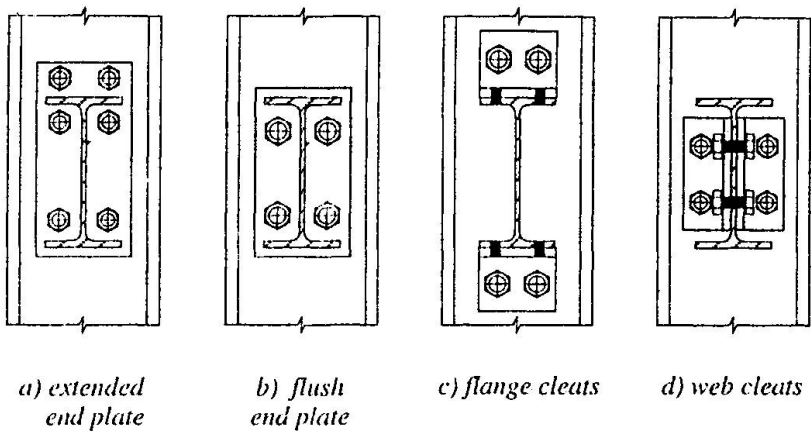


Fig. 1. Beam-to-I section column minor-axis joints

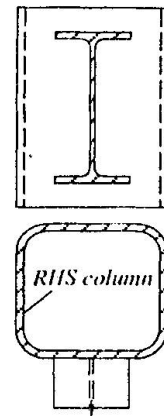


Fig. 2. Beam-to-RHS column joint

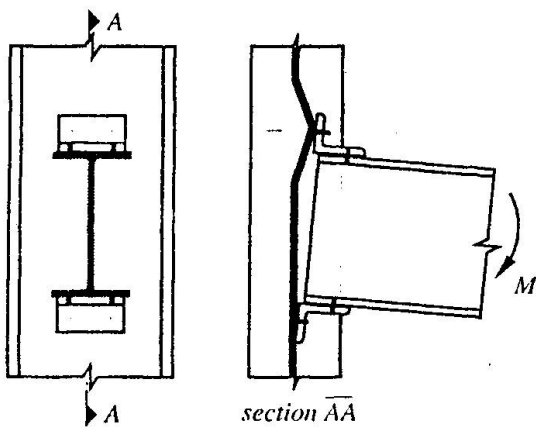


Fig. 3. Local mechanism

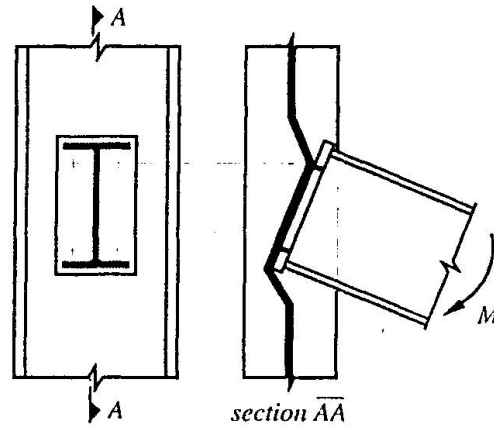


Fig. 4. Global mechanism

2. Local failure

2.1 Flexural mechanisms

Basic failure mechanisms are obtained by the Johansen yield line method, using log-spiral fans in order to optimise the yield line pattern. The plastic moment per unit length of yield line is given by

$$m_{pl} = 0,25 t_w^2 f_y \tag{1}$$

(f_y = yield stress; t_w = thickness of the column web).

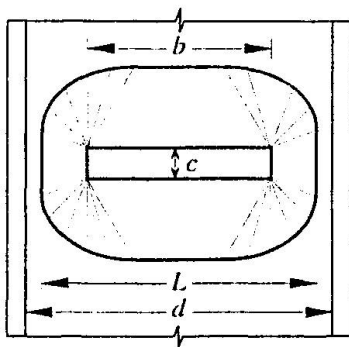


Fig. 5. Yield line pattern (Local mechanism)

In the flexural mechanisms, it is assumed that the plastic moment is not reduced by the presence of shear force perpendicular to the plane of the web; this reduction is taken into account in section 2.3. The plastic failure load associated to the optimised mechanism of Fig. 5, for F acting on a rectangle $b \times c$ (loading case 1), is given by

$$F_{pl} = 4\pi m_{pl} \left(1 + \frac{4}{\pi} \cot\theta + \cot^2\theta + \frac{2c}{\pi(L-b)} \right),$$

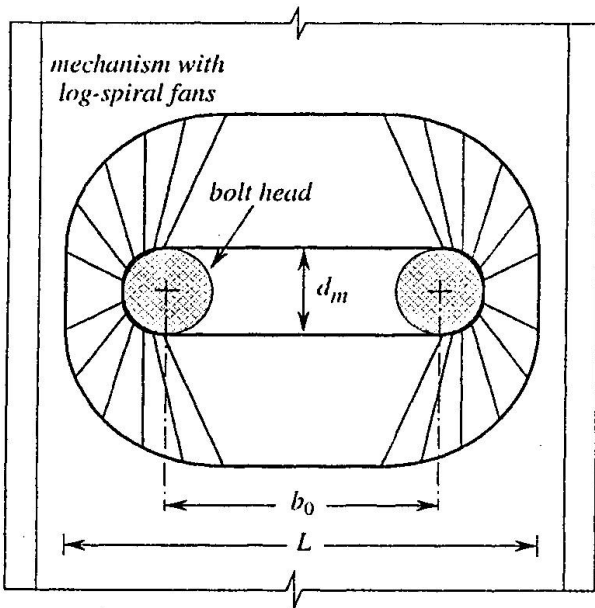
where θ is the solution of the equation $\frac{b}{L-b} = 2 e^{\frac{\pi}{2} \cot \theta} \cot \theta$, and $L = d - 1,5r$.

For practical design purposes it is desirable to make use of a simplified formula, explicit in F_{pl} , which may be given by the approximate solution

$$F_{pl} = \frac{4\pi m_{pl}}{1 - \frac{b}{L}} \left(\sqrt{1 - \frac{b}{L}} + \frac{2c}{\pi L} \right) \quad (2)$$

For the loading case 2 (e.g. Fig. 6), the mean diameter of the bolt head, Fig. 7, is defined by

$$d_m = \frac{d_1 + d_2}{2} \quad (3)$$



The yield line mechanism of Fig. 6 leads to the plastic load

$$F_{pl} = \frac{4\pi m_{pl}}{1 - \frac{a^*}{L-b_1}} \left(1 + \frac{4}{\pi} \cot \theta + \cot^2 \theta \right),$$

where $a^* = d_m e^{-\frac{\pi}{2} \cot \theta}$,

$$b_1 = b_0 + d_m \left(1 - e^{-\frac{\pi}{2} \cot \theta} \right),$$

and θ is the solution of the equation

$$\frac{b_1}{L-b_1} = 2e^{\frac{\pi}{2} \cot \theta} \cot \theta .$$

Instead of this complex system of equations, the simplified formula (2) may also be used for the evaluation of the failure load in the tension zone, Fig. 8, if this zone is replaced by an equivalent rectangle with the dimensions:

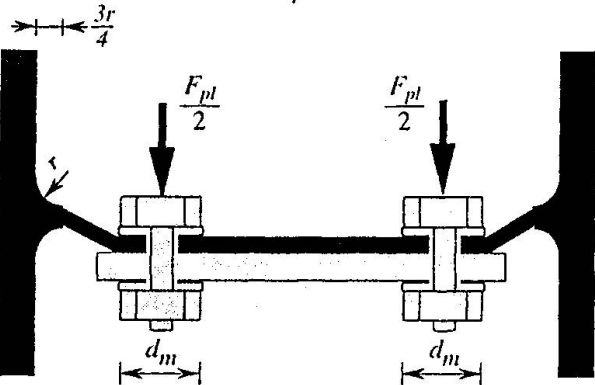


Fig. 6. Failure mechanism of bolted connection

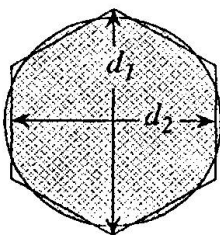


Fig. 7. Bolt head (or nut)

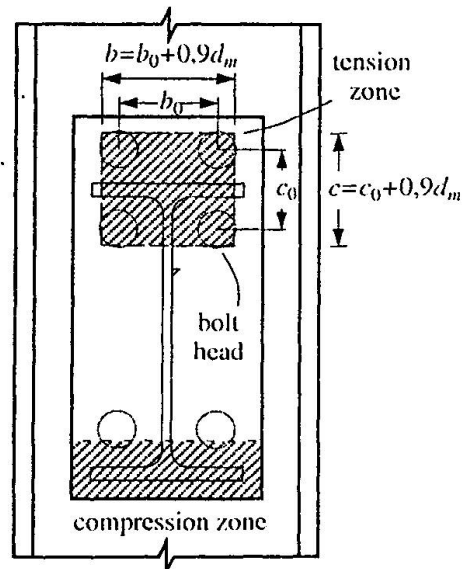


Fig. 8. Bolted connection



$$\begin{cases} b = b_0 + 0,9d_m \\ c = c_0 + 0,9d_m \end{cases} \quad (4)$$

The same formula (2) may therefore be used in the two loading cases.

2.2 Punching shear mechanisms

For the *loading case 1* the punching perimeter is a rectangle with the dimensions $b \times c$. The punching load is then given by

$$F_{punch} = 2(b + c) v_{pl}, \quad \text{where } v_{pl} = t_w f_y / \sqrt{3}. \quad (5)$$

For the *loading case 2* the punching of the column web around each bolt head must be checked. If there are n bolts in the tension zone, the punching load is given by

$$F_{punch} = n \pi d_m v_{pl}. \quad (6)$$

2.3 Combined flexural and punching shear mechanisms

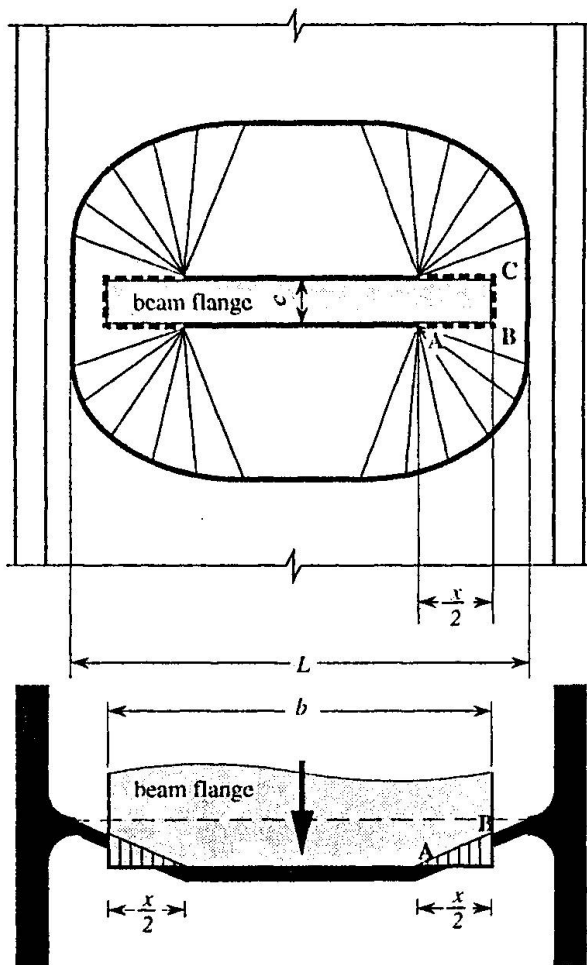


Fig. 9. Combined flexural and punching shear failure

A combined flexural and punching shear mechanism presents not only flexural yield lines (thick lines in Fig. 9) but also punching shear yield lines (dotted lines in Fig. 9). Packer *et al* [2] proposed similar combined failure modes using straight lines or circular fans, instead of the optimised mechanism of Fig. 9 that uses log-spiral fans.

The present solution also takes into account that the plastic moment per unit length of yield line is reduced by the presence of shear when v (the shear force per unit length)

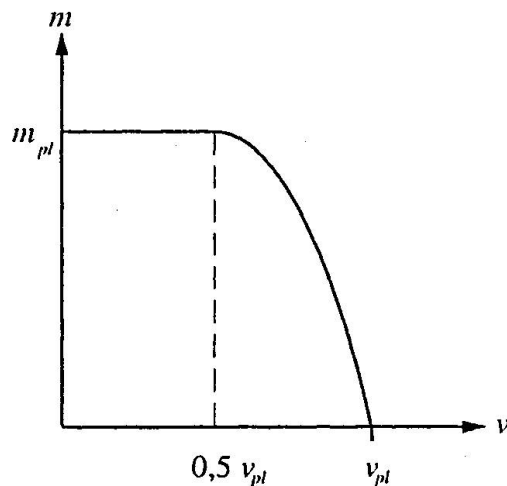


Fig. 10. Interaction between m (moment) and v (shear force)



exceeds 50% of v_{pl} , according to the interaction diagram of Fig. 10. This provides a refinement of the previous solution proposed by the authors [3]. In spite of the refinement, the expression for the plastic load is presented in a simpler form (avoiding the iterative procedure of the previous solution):

$$F_{Q2} = 4 m_{pl} \left[\frac{\pi \sqrt{L(a+x)} + 2c}{a+x} + \frac{1,5 c x + x^2}{\sqrt{3} t_w (a+x)} \right], \quad (7)$$

where: $a = L - b$,

$$\begin{cases} x = 0 & \text{if } b \leq b_m \\ x = -a + \sqrt{a^2 - 1,5 ac + \frac{\sqrt{3} t_w}{2} [\pi \sqrt{L(a+x_0)} + 4c]} & \text{if } b \geq b_m \end{cases}$$

$$x_0 = L \left[\left(\frac{t}{L} \right)^{\frac{2}{3}} + 0,23 \frac{c}{L} \left(\frac{t}{L} \right)^{\frac{1}{3}} \right] \left(\frac{b - b_m}{L - b_m} \right)$$

$$\text{and } b_m = L \left[1 - 0,82 \frac{t_w^2}{c^2} \left(1 + \sqrt{1 + 2,8 \frac{c^2}{t_w L}} \right)^2 \right], \text{ but } b_m \geq 0, \quad (8)$$

Equation (7) provides an additional advantage with respect to the previous solution [3]: it may be applied in the full range $0 \leq b \leq L$, instead of the previous constraint $b \leq 0,8L$.

For the *loading case 2* (bolted connections) the equivalent rectangle, defined by equation (4), may be used.

2.4 Correction to take into account the difference between Johansen and Von Mises yield criteria

The plastic failure loads obtained by the yield line method differ from the exact solutions based on the Von Mises yield criterion. It was shown [5] that if $(b+c)/L \geq 0,5$ the optimised yield line mechanisms provide an accurate solution. However, if $(b+c)/L < 0,5$, the yield line method overestimates the plastic load. The influence of the yield criteria on the plastic load was evaluated by numerical simulations performed with the finite element program

FINELG [4] that uses the Von Mises yield criterion, instead of the square yield criterion (Fig. 11) used in the Johansen yield line method.

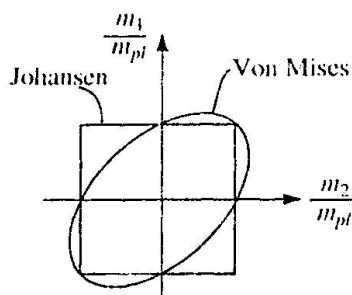


Fig. 11. Yield criteria for plates (m_1, m_2 - principal moments)

Final expressions for flexural mechanism as well as for combined mechanism should then include a correction factor k that multiplies Eq. (2) or Eq.(7) in order to obtain an accurate plastic load. The correction factor k may be evaluated as [5]:

$$k = \begin{cases} 1 & \text{if } (b+c)/L \geq 0,5 \\ 0,7 + 0,6(b+c)/L & \text{if } (b+c)/L \leq 0,5 \end{cases} \quad (9)$$



2.5 Comparison between the three modes of local failure

It is obvious that equations (7) and (2) are identical when $x = 0$ (no punching), meaning that the combined mechanism is transformed into the pure flexural mechanism. This occurs when $b \leq b_m$, where b_m is the particular value of b that determines the boundary between the two mechanisms. When $b > b_m$ equation (7) gives a plastic load always smaller than equation (2), which means that equation (2) is useless.

The local failure mechanism is the mechanism associated to the lowest plastic load which is then given by

$$F_{local} = \min(F_{punch}; k F_{Q2}). \quad (10)$$

The three modes of local failure are compared in Fig. 12 for a bolted connection with two bolts in the tension zone, like that of Fig. 6. The bolted diameter is fixed to $d_m = 0,1L$, and from equation (4) the equivalent rectangle is defined by $b = b_0 + 0,09L$ and $c = 0,09L$. Fig. 12 shows the variation of the failure load (thick line) as a function of b , representing the three modes of failure.

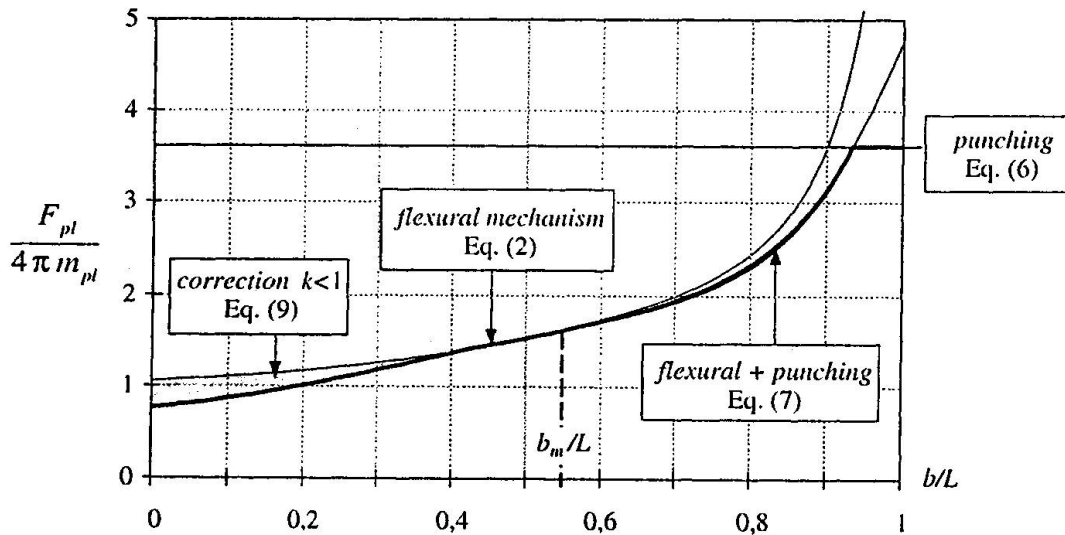


Fig. 12. Comparison between the three modes of local failure

3. Global failure

The global failure load, for flexural mechanisms or for combined flexural and punching mechanisms, may be evaluated as

$$F_{global} = \frac{k F_{Q2}}{2} + m_{pl} \left(\frac{2b}{h} + \pi + 2\rho \right), \quad (11)$$

where F_{Q2} and k are given by equations (7) and (9), h is the distance between centres of compression and tension zones, and ρ is given by

$$\begin{cases} \rho = 1 & \text{if } 0,7 \leq \frac{h}{L-b} \leq 1 \\ \rho = \frac{h}{L-b} & \text{if } 1 \leq \frac{h}{L-b} \leq 10 \end{cases}$$

Outside the range $0,7 \leq \frac{h}{L-b} \leq 1$ equation (11) is no more valid. However it underestimates the plastic load if the following values of ρ are assumed:

$$\begin{cases} \rho = 1 & \text{for } \frac{h}{L-b} < 0,7 \\ \rho = 10 & \text{for } \frac{h}{L-b} > 10 \end{cases}$$

Global failure mechanisms involve both compression and tension zones, Fig. 4. These mechanisms are assumed to be symmetrical with respect to a horizontal and to a vertical axis in the plane of the column web. The horizontal symmetry is not an exact assumption when the dimensions $b \times c$ of the compression zone are different from those of the tension zone, e.g. Fig. 8. In this case equation (11) should be applied separately for each zone, leading to two different loads, and the failure load will be an intermediate value. However the two zones are often assumed to be equal (see section 4) and then equation (11) will be applied only once.

4. Ultimate moment

The ultimate moment is finally obtained by $M_{pl} = h \times \min(F_{local}, F_{global})$ where h is the distance between centres of compression and tension zones. It may be assumed, in common cases, that the beam only transmits moment to the column (no axial force in the beam) which means that the compression and tension forces are equal. Referring to the connection in Fig. 8, the tension force is first evaluated and, as the compression force is equal to the tension force, the dimension c of the compression zone will be determined in order to have the same plastic load. As an alternative to this determination of h , a direct evaluation of this value may be obtained by assuming that compression and tension zones have the same dimensions $b \times c$.

In some situations (e.g. Fig. 13), h , and b are known, but c is indeterminate. From the condition of moment maximisation with respect to c , the following c may be obtained:

$$c = h, \left(0,3 \frac{b}{L} + 0,1 \frac{h}{L} - 0,15 \right) \text{ but } 0 < c < 0,5h.$$

5. Conclusions

The evaluation of the moment capacity of minor-axis joints is a complex task due to the large number of failure modes of the column web. The proposed method, however, predicts these failure modes with few expressions, easy to use by designers. Comparisons of theoretical predictions with 12 experimental tests [6] and with a large number of numerical simulations [7] confirm the accuracy of the analytical method. Details on the background of this method may be found in [8].

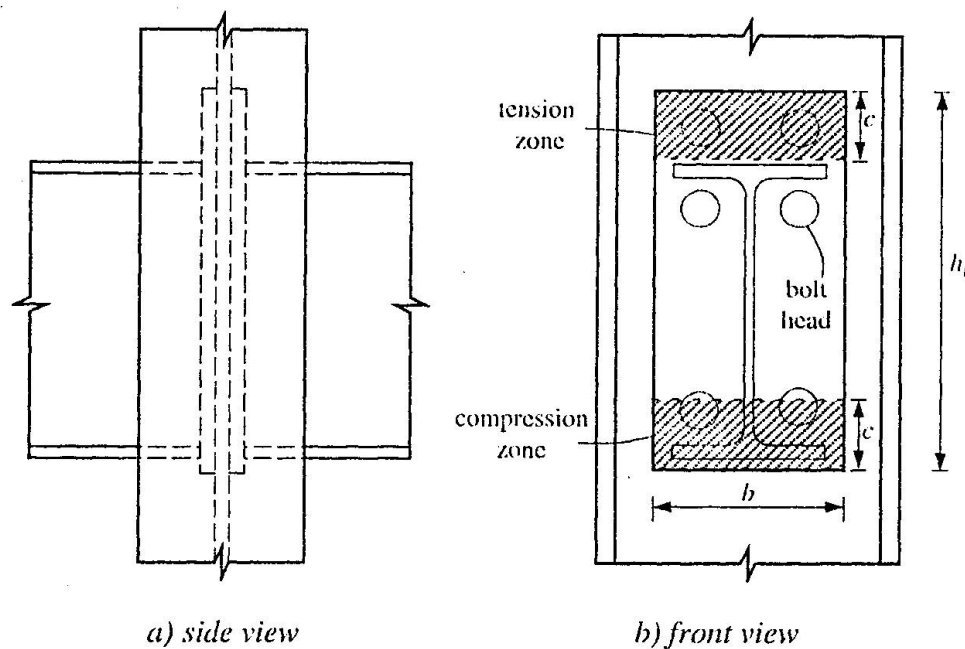


Fig. 13. Joint with two beams one of each side of the column web

References

- [1] Eurocode 3 - *Design of steel structures*, part 1-1, General rules and rules for buildings, CEN, ENV 1993-1-1, 1992, Including Revised Annex J - *Joints in building frames*, 1994.
- [2] Packer, J. A., Morris, G. A. and Davies, G. - *A Limit state design method for welded tension connections to I-sections webs*, J. of Constructional Steel Research, Vol. 92, 1989, pp. 33-53.
- [3] Gomes, F. C. T., Jaspart, J.-P., Maquoi, R. - *Behaviour of minor-axis joints and 3-D joints*, Proceedings of the Second State of the Art Workshop COST C1 on Semi-rigid Connections, Ed.: F. Wald, Czech Technical University, Prague, 26 - 28.10.1994. pp. 111-120.
- [4] Frey, F., De Ville de Goyet V., et al. - *FINELG - Non-linear Finite Element Analysis Program - User's Manual Version 5.2*, University of Liège, March, 1990.
- [5] Gomes, F. C. T. - *État limite ultime de la résistance de l'âme d'une colonne dans un assemblage semi-rigide d'axe faible*, Internal Report N^o. 203, Dept. MSM, University of Liège, 1990.
- [6] Gomes, F.C.T., Jaspart, J.-P. - *Experimental research of minor-axis joints. Comparison with theoretical predictions*, COST C1 - WG2 "Steel and Composite" Meeting, Doc. C1/WD2/94-13, Coimbra, 25 - 26.11.1994.
- [7] Neves, L.F.C., Gomes, F.C.T. - *Semi-rigid behaviour of beam-to-column minor-axis joints*, IABSE Colloquium, Istanbul, 25 - 27.09.1996.
- [8] Gomes, F. C. T. - *Comportement semi-rigide de nœuds poutre-colonne d'axe faible et résistance de nœuds tridimensionnels en acier*, Doctoral thesis (to be submitted at the University of Liège).

Conceptual design of joints in braced steel frames

Martin STEENHUIS Research Assistant TNO Building and Construction Research Delft The Netherlands	Harry EVERS Director ECCS bv Hoofddorp The Netherlands	Nol GRESNIGT Senior Lecturer University of Technology Delft The Netherlands
---	---	--

Summary

To help practitioners to find the most economical design of braced frames, this paper proposes a classification of joints in 'simple' (e.g. web cleated connections), 'moderate' (e.g. flush end plated connections) and 'complex' (e.g. stiffened extended end plate connections) with respect to the fabrication complexity (low, medium and high costs). Different types of joints are classified into the three aforementioned classes in a table format. This enables a practitioner to simply read the class of a given joint from the table, without calculation. For each class, recommendations are given what strength and what stiffness should be used during the conceptual design stage of the frame. Furthermore, the paper shows that, during the final design of the braced frame, the recommended stiffness values can be used safely without further checks. In other words, there is no need to determine the 'actual' stiffness of the joint during final design, which lightens the design task dramatically. What remains is a check of the strength and, in case of plastic frame analysis, the rotation capacity.

A comparison of frame alternatives is included, which demonstrates that application of moderate joints compared to simple joints may be economical due to savings in beam costs.

List of symbols

- b_{eff} is the effective width of the column web in compression;
 f_y is the yield strength;
 k_x is a stiffness factor dependent from the type of joint relative to the lever arm;
 $k_{x,\text{act}}$ is a stiffness factor dependent on the 'actual' stiffness of a specific joint;
 $k_{x,\text{app}}$ is a stiffness factor dependent on the type of joint relative to the beam depth;
 l_b is the beam span;
 $t_{f,c}$ is the column flange thickness;
 $t_{w,c}$ is the column web thickness;
 z is the distance between centre of compression and tension;
 k_y is a strength factor dependent on the type of joint relative to the lever arm;
 E is the Young's modulus;
 F_c is the design capacity of the column web in compression;
 I_b is the moment of inertia of the beam;
 M_{Rd} is the design moment capacity of a joint;
- S_j is the initial stiffness;



$S_{j,act}$ is the initial stiffness calculated according to Eurocode 3 or another design standard;
 $S_{j,app}$ is the 'good guess' of the initial stiffness;
 γ_{M0} is the partial safety factor for members.

1. Classification of joints with respect to fabrication complexity

Eurocode 3 [1] presents two classification schemes for the design of joints with respect to strength and stiffness. For elastic frame analysis, the stiffness classification in 'nominally pinned', 'semi rigid' and 'rigid' may be used. For plastic frame analysis, the strength classification in 'nominally pinned', 'partial strength' and 'full strength' may be used.

Anderson et al. [2] demonstrated that braced frames with nominally pinned joints require heavier beams than frames with semi rigid, partial strength joints. They may be economical due to low fabrication costs of the joints. Dependent on beam span and fabricator, frames with semi rigid, partial strength joints may also be economical. In that case the economy is achieved by lower beam costs (despite higher costs for the joints). Frames with rigid and/or full strength joints are uneconomical due to high fabrication costs of the stiffened joints.

Gibbons [3] showed that alternatives for braced frames can be distinguished in terms of 'simple', 'moderate' and 'complex' with respect to their fabrication complexity. In this paper, we will use these terms in a classification system for joints. Possible economical solutions are braced frames with simple joints or braced frames with moderate joints. Table 1 shows the link between the classification with respect to the fabrication complexity and the Eurocode 3 classification. The grey cells in this table indicate the economical alternatives.

Tab. 1. Classification with respect to fabrication complexity compared to Eurocode 3

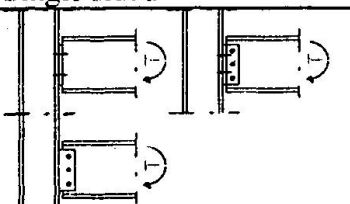
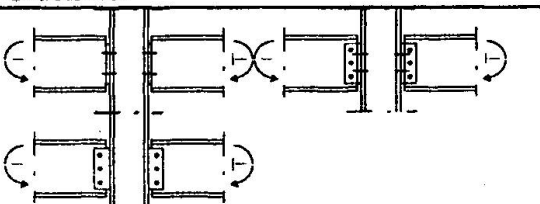
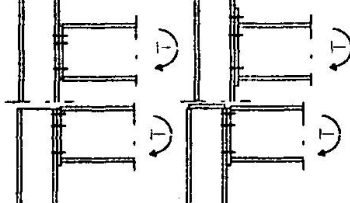
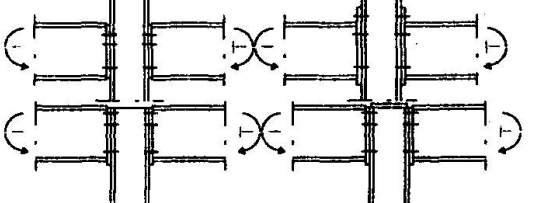
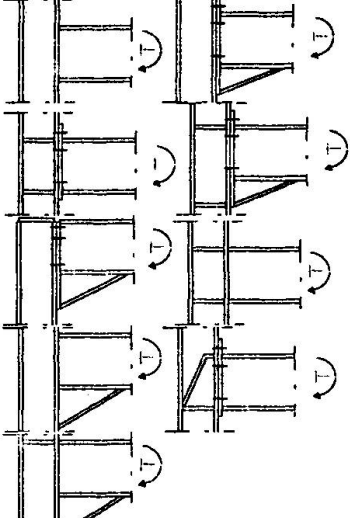
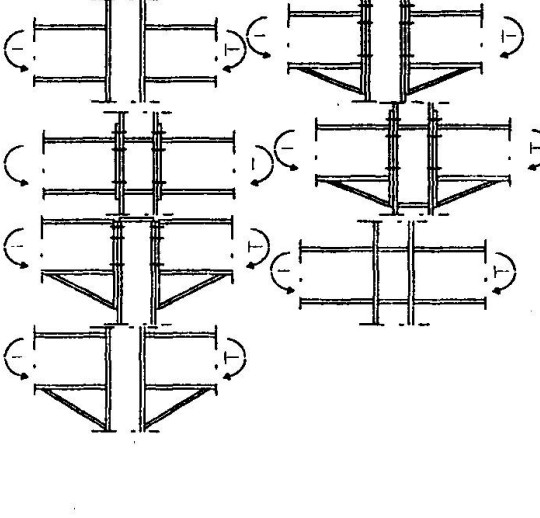
Classification with respect to fabrication complexity	Stiffness classification according to Eurocode 3	Strength classification according to Eurocode 3
Simple	Nominally pinned	Nominally pinned
Moderate	Semi rigid (but unstiffened)	Partial strength (but unstiffened)
Complex	Semi rigid (but stiffened) or Rigid	Partial strength (but stiffened) or Full strength

Table 2 shows how different types of joints are classified in simple, moderate and complex. Simple joints are those types of joints which are traditionally treated as nominally pinned, for example joints with flexible end plates, fin plates or web angle cleats. Moderate joints are for example joints with end plates. Complex joints are welded joints and stiffened joints with end plates. The welded joints have been shifted to the complex class, due to the costs of welding on site.

The background of the proposed classification is as follows. In various European countries, traditionally, two parties are responsible for the design of steel frames: the engineer designs the beams and columns and the steel fabricator designs the joints. In this design practice, the engineer specifies the mechanical requirements of joints. The steel fabricator designs the joints to fulfil these requirements. The fabricator also considers manufacturing aspects.

In this design practice, the use of simple joints is favoured, because the engineer can design beams and columns without knowledge of the lay out of the joints. The joints normally will be designed in a subsequent step by the steel fabricator based on the results of the frame analysis.

Tab. 2. Types of joints classified with respect to fabricational complexity

Class	Single sided	Cruciform
Simple		
Moderate		
Complex		

Ideally, for moderate and complex joints, it would be best if beams, columns and joints are designed by one single party (allowing the mechanical properties of the joints to be introduced in the frame analysis). As explained before, this is not current practice. Therefore, there is a need for simple design recommendations for engineers to assess the strength and stiffness requirements of moderate joints. These requirements should allow a steel fabricator to design economical joints.

In this paper, a proposal for the design recommendations is given. The scope of this paper is restricted to European H and I sections. It is assumed that the beam depth is greater than or equal to the column depth. Some further restrictions apply to end plated joints:

- a connection has two bolt rows in tension;
- the bolt diameter is approximately 1.5 times the thickness of the column flange;



- the location of the bolt is close to the root radius of the column flange, the beam flange and the web;
- the end plate thickness is similar to the column flange thickness.

In section 2, stiffness classification criteria are given to be used during elastic frame analysis. Section 3 focuses on strength classification criteria for plastic frame analysis. In the last section, a practical example demonstrates the benefits of the given recommendations.

2. Stiffness classification criteria

In this section, criteria are given as to what stiffness should be introduced in the frame analysis for each class of joints (simple, moderate or complex). These criteria are based on the work of Steenhuis, Gresnigt and Weynand in [4]. They presented a design method for elastic design allowing the frame to be designed by an engineer and the (semi rigid) joints to be designed by a steel fabricator. The design method is identical to the traditional design process for nominally pinned or rigid joints, but:

- instead of assuming that a joint is nominally pinned or rigid, the initial stiffness of the joint is assessed by means of a 'good guess'. For this 'good guess' only information is required about the connected beam and column and an impression about the type of joint;
- the agreement between the 'good guess' and the 'actual' stiffness (the design initial stiffness) of the joint needs to be verified. This is similar to the concept of checking that a joint is rigid.

The 'good guess' can be made with the help of the following formula:

$$S_{j,app} = \frac{E z^2 t_{fc}}{k_x} \quad (1)$$

Factor k_x can be read from table 3 for a limited number of joints.

Tab.3. k_x - factor for beam to column joints (taken from [4])

Single sided	k_x	Cruciform	k_x
	13		7,5
	8,5		3
	5,5		0

In the case of braced frames, the agreement between the 'good guess' ($S_{j,app}$) and the 'actual' stiffness ($S_{j,act}$) of the joint can be verified with:

$$\text{In case } S_{j,app} < \frac{8 E I_b}{l_b} \text{ then } \frac{8 S_{j,app} E I_b}{10 E I_b + S_{j,app} l_b} \leq S_{j,act} \leq \frac{10 S_{j,app} E I_b}{8 E I_b - S_{j,app} l_b} \quad (2)$$



$$\text{else } \frac{8 S_{j,\text{app}} E I_b}{10 E I_b + S_{j,\text{app}} I_b} \leq S_{j,\text{act}} \leq \infty \quad (3)$$

If these requirements are fulfilled, the bearing capacity (column buckling load) of a frame with joint stiffness $S_{j,\text{act}}$ will differ less than 5% from the same frame with joint stiffness $S_{j,\text{app}}$. For backgrounds to these formulae, we refer to [4].

In section 2.1 we will investigate whether instead of k_x -factors for each type of joint, we then can give k_x -factors for each class of joint. We expect that this is possible due to the fact that the response of braced frames is relatively insensitive to variations in stiffness.

2.1 Sensitivity of a braced frame to variations in stiffness

When we know $S_{j,\text{app}}$, boundaries for the allowed variation of $S_{j,\text{act}}$ are given with equations (2) and (3). We will now investigate whether these criteria can be presented in a manageable format, in order to draw some conclusions concerning the sensitivity of a braced frame to variations in stiffness. For the sake of simplicity we only focus on the situation that $S_{j,\text{app}} < \frac{8 E I_b}{I_b}$.

The approximate stiffness $S_{j,\text{app}}$ can be determined with equation (1). We can remove z from this equation by defining:

$$k_{x,\text{app}} = k_x \frac{h_b^2}{z^2} \quad (4)$$

This yields to the following result:

$$S_{j,\text{app}} = \frac{E h_b^2 t_{f,c}}{k_{x,\text{app}}} \quad (5)$$

The expression for allowable variation in stiffness (equation (2)) can be rewritten as:

$$\frac{8}{10 + \frac{h_b^2 t_{f,c}}{k_{x,\text{app}} I_b}} \leq \frac{k_{x,\text{app}}}{k_{x,\text{act}}} \leq \frac{10}{8 - \frac{h_b^2 t_{f,c}}{k_{x,\text{app}} I_b}} \quad (6)$$

The frame response is sensitive to variations in joint stiffness when the beam is stocky. Hence we take $h_b = 15 h_b$.

$$\frac{8}{10 + \frac{15 h_b^3 t_{f,c}}{k_{x,\text{app}} I_b}} \leq \frac{k_{x,\text{app}}}{k_{x,\text{act}}} \leq \frac{10}{8 - \frac{15 h_b^3 t_{f,c}}{k_{x,\text{app}} I_b}} \quad (7)$$

From formula (7) it appears that for small values of $t_{f,c}$, the frame is sensitive to variations in $k_{x,\text{app}}$. We use $\frac{h_b^3 t_{f,c}}{I_b} = 4$ as a lower bound for frames with stocky beams and slender columns.

This leads to:

$$0,8 k_{x,\text{app}} - 6 \leq k_{x,\text{act}} \leq 1,25 k_{x,\text{app}} + 7,5 \quad (8)$$

If $k_{x,\text{app}} < 7,5$, the joint is rigid. Figure 1 shows this expression in a graphical form. From this graph, we can conclude that the response of a braced frame is insensitive to variations in stiffness of the joints. For example, if $k_{x,\text{app}} = 13$, the 'actual' stiffness may be up to $13/23,75 = 0,55$ times lower and up to $13/4,4 = 2,95$ times higher. The value $k_{x,\text{app}} = 13$ corresponds for example to a joint with an extended end plate (single sided). This enormous variation is despite the worst case assumptions we did when deriving the relation between $k_{x,\text{app}}$ and $k_{x,\text{act}}$.

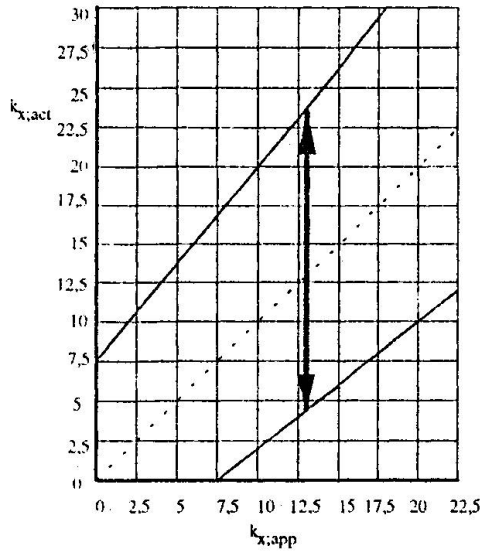


Fig. 1. $k_{x,act}$ as function from $k_{x,app}$

Since variations in stiffness have such a limited influence on the frame behaviour, stiffness criteria can be given as in table 4, where different types of joints are grouped in three classes. The chosen stiffness for each class of joints is rather low for two reasons:

- the moments found during elastic analysis will be lower. Therefore there is more chance to find an economical solution;
- when the 'actual' stiffness is higher than the 'good guess', deformations will be smaller and the frame bearing capacity (column buckling load) will be higher. This is on the safe side.

Tab. 4. Stiffness classification of joints in braced frames for predesign

Class	Single sided	Cruciform
	S_j	S_j
Simple	0	0
Moderate	$\frac{E h_b^2 t_{fc}}{22}$	$\frac{E h_b^2 t_{fc}}{13}$
Complex	$\frac{E h_b^2 t_{fc}}{11}$	$\frac{E h_b^2 t_{fc}}{6.5}$

If the approximate stiffness $S_{j,app}$ (adopted in the frame analysis) is low compared to the 'actual' stiffness $S_{j,act}$, the joints should have sufficient rotational capacity to allow for some plasticity. Eurocode 3 [1] gives some guidance. As a general rule, we recommend to design the welds for the full moment capacity of the joints. For an end plate or a column flange in bending, yielding of the plate or flange is the preferred failure mode.

2.2 Need for stiffness verifications

Now we will investigate whether there is a need to verify the agreement between the stiffness design recommendations given in table 4 and the 'actual' stiffness.

In this verification we used information from design tables [5, 6] according to Eurocode 3. Types of joints investigated are:

- single sided flush end plate joints, see figure 2;
- single sided extended end plate joints, see figure 3;
- cruciform extended end plate joints, see figure 4;
- cruciform welded joints, see figure 5.

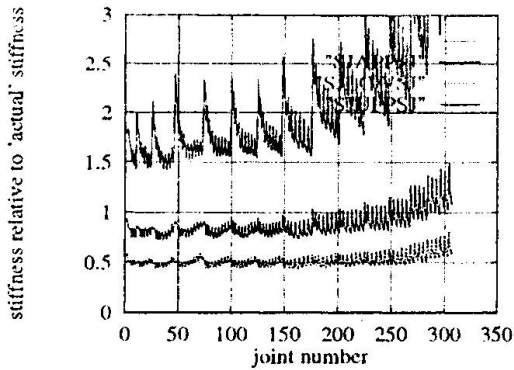


Fig. 2. Single sided flush end plate joints (moderate)

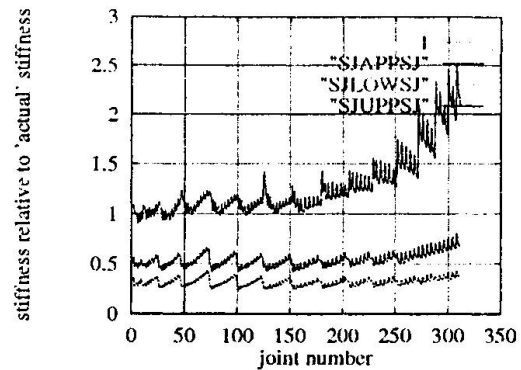


Fig 3. Single sided extended end plate joints (moderate)

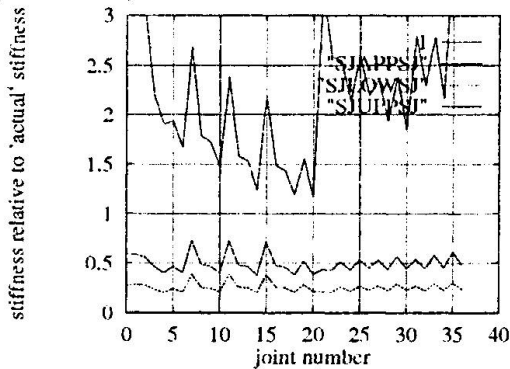


Fig 4. Cruciform extended end plate joints (moderate)

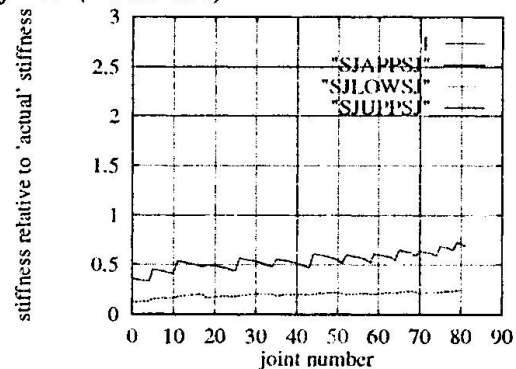


Fig 5. Cruciform welded joints (complex)

Figures 2 to 5 show each four lines:

- '1'. This line represents the case that $S_{j,app}$ equals $S_{j,act}$;
- 'SJAPPSJ'. This line represents $S_{j,app}$ divided by $S_{j,act}$;
- 'SJLOWSJ'. This line represents the lower bound for the 'actual' stiffness $\left(\frac{8 S_{j,app} E I_b}{10 E I_b + S_{j,app} l_b}\right)$ divided by $S_{j,act}$. For the lower bound, see equation (2) and (3);
- 'SJUPPSJ'. This line represents the upper bound for the 'actual' stiffness $\left(\frac{10 S_{j,app} E I_b}{8 E I_b - S_{j,app} l_b}\right)$ or ∞ divided by $S_{j,act}$. For the upper bound, see equation (2) or (3).

The approximate stiffness $S_{j,app}$ is calculated according to table 4 and the 'actual' stiffness $S_{j,act}$ is read from the design tables [5, 6]. The horizontal axis represents the different joints in consecutive order. Conservatively it is assumed that the beam span is 15 times the beam depth.

It appears in all cases that none of the lower bounds is crossing the line '1'. Only few joints touch the upper bound, which means that possibly an additional safety of 5% has been



achieved in these cases. It can be concluded that the classification scheme can be used without formal check of the stiffness.

3. Strength classification criteria

In section 2 we introduced stiffness criteria for a classification system for joints in braced frames with respect to the fabrication complexity. This system consists of stiffness recommendations for different classes of joints to be adopted during frame analysis. It is suitable for elastic frame analysis.

When adopting plastic frame analysis or when verifying the strength of joints after elastic analysis has been carried out, it could be helpful for a designer to have a quick impression of the moment capacity of different joint types. In analogy to the prediction formula for stiffness [4], a formula can be derived to make a first approximation of the joint strength. This formula has the form:

$$M_{Rd} = k_y f_y z t_{fc}^2 / \gamma_{M0} \quad (9)$$

Factor k_y is dependent on the type of failure expected in the joint. For an unstiffened single sided joint, this is for example column web in shear, for an unstiffened cruciform joint, this is for example column web in compression or tension. It is assumed that bolt failure or end plate in bending is not the governing failure mode in the joint.

Determination of k_y , see also [4], for a joint failing due to column web in compression:

$$M_{Rd} = F_c z \approx \frac{f_y b_{eff} t_{w,c} z}{\gamma_{M0}} \approx \frac{f_y 12 t_{fc} 0,6 t_{fc} z}{\gamma_{M0}} \approx \frac{7,2 f_y z t_{fc}^2}{\gamma_{M0}} \quad (10)$$

The value of k_y has been determined by calculating $M_{Rd} / (f_y z t_{fc}^2 / \gamma_{M0})$ for a number of joints from the design tables [5, 6]. This has been reported in figures 6 and 7. The joints selected in figure 6 fail due to shear of the column web. The joints selected in figure 7 fail due to column web in compression. We choose: $k_y = 5$ (single sided joint) and $k_y = 7$ (cruciform joint).

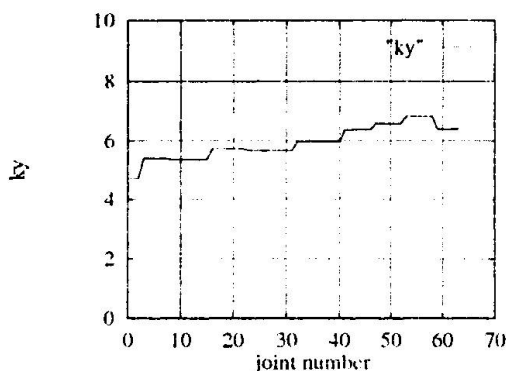


Fig 6. Unstiffened extended end plate joints failing in shear

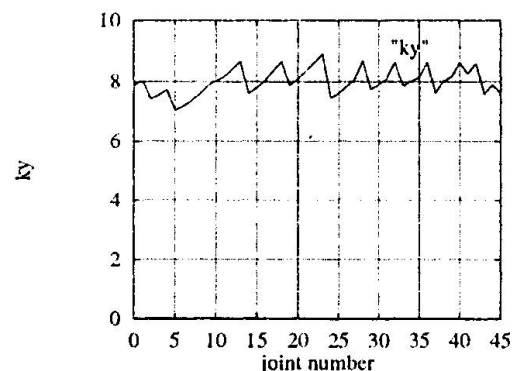


Fig 7. Unstiffened welded joints failing in compression or tension

For two reasons, the approximation formula for strength is not as accurate as the stiffness formula. Firstly, there is the direct impact of the strength of the joint on the frame behaviour. Secondly, the formula is based on a specific failure mode (e.g. column web in shear) of the joint. In reality, another failure mode may govern the joint behaviour. Therefore, the approximation formula can only be used in a first design step. Strength verifications according

to the code always have to be carried out after a joint has been designed. We present design recommendations in table 5. With the help of this table, a designer can quickly check whether a certain solution runs into costs.

Tab. 5. Strength recommendations for joints in braced frames during predesign.

Class	Single Sided	Cruciform
	M_{Rd}	M_{Rd}
Simple	()	()
Moderate	$\leq 5 f_y z t_{fc}^2 / \gamma_{M0}$	$\leq 7 f_y z t_{fc}^2 / \gamma_{M0}$
Complex	$> 5 f_y z t_{fc}^2 / \gamma_{M0}$	$> 7 f_y z t_{fc}^2 / \gamma_{M0}$

4. Example

In this example, the difference in costs between two frames has been determined. It concerns a frame with simple joints and a frame with moderate joints. Figure 8 shows the lay out of the frames. In the frame with simple joints, web angle cleat connections have been adopted. In the frame with moderate joints, full depth end plates have been used, see figure 9. Full details of the design are given in [7].

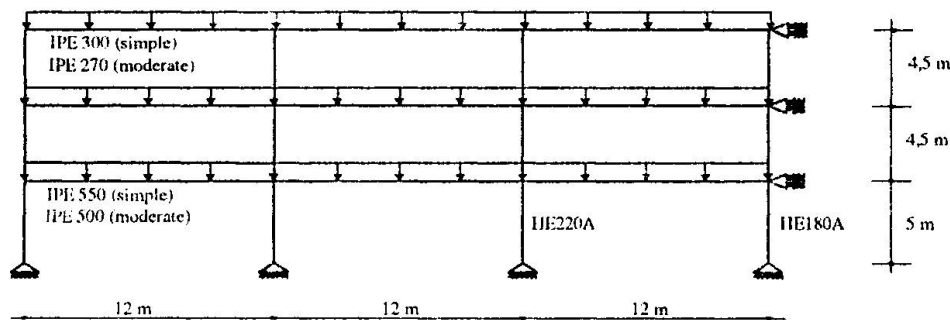


Fig 8. Geometry of frame

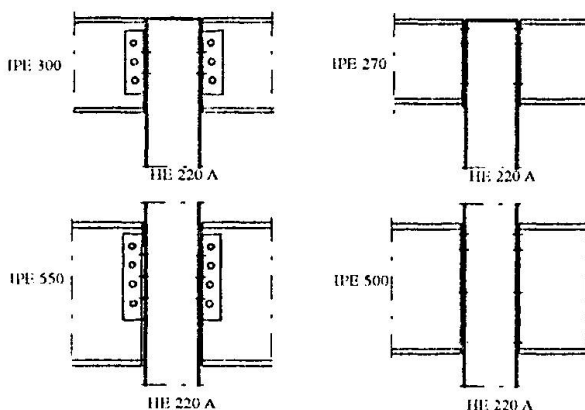


Fig 9. Simple and moderate joints

Table 6 gives the cost breakdown in Dutch guilders for 5 frames. It can be concluded from the table the total costs of the frames with moderate joints are lower than the costs of the simple



frames. Despite higher fabrication costs, this is due to materials savings, lower assemblage costs and savings in anti corrosion measures.

Tab. 6. Costs comparison of frames, (in guilders)

Category	Simple	Moderate	Simple compared to moderate
Material	65.724	54.791	120%
Production	12.103	17.278	70%
Anti Corrosion	19.520	18.192	104%
Assemblage	16.800	12.800	131%
Engineering	6.124	7.164	85%
Unforeseen (10%)	12.027	11.022	
total	132.298	121.247	109%

Conclusions

Joints in braced frames can be classified in terms of simple, moderate and complex with respect to fabrication aspects. For these classes, we established design recommendations for both stiffness and strength. These recommendations can be used during frame design. For stiffness, values are given to be introduced in the frame analysis. These values are in good agreement with the 'actual' stiffness of joints from a certain class. For strength, simple criteria have been derived to find out in what class specific joints will fall.

References

- [1] EUROCODE 3, ENV - 1993-1-1, *Revised annex J*, Design of Steel Structures, CEN, European Committee for Standardization, Document CEN / TC 250 / SC 3 - N 419 E, Brussels, Belgium, June 1994.
- [2] ANDERSON D., COLSON A., JASPART J.-P., *Frame Design and Economy*, ECCS TWG 10.2 Publication, Bouwen met Staal 117, page 34-38, SBI Rotterdam, The Netherlands, March 1994. Also published in other National Steel Journals.
- [3] GIBBONS, C, *Economic Steelwork Design*, The Structural Engineer, Volume 73/No 15, London, United Kingdom, August 1995
- [4] STEENHUIS M., GRESNIGT N., WEYNAND K., *Predesign of semi rigid joints in steel frames*, proceedings of the second workshop on semi rigid connections, edited by F. Wald, Technical University of Prague, Czech Republic, October 1994.
- [5] SPRINT RA 351, *Design Tables*, CTICM, St Rémy-lès-Chevreuse, France, 1995
- [6] WALD F., *Connection Design Tables to ENV 1993-1-1 (Eurocode 3)*, Technical University of Prague, Czech Republic, April 1994.
- [7] DOL. C., STEENHUIS M., *Bolted end plate connections (in Dutch)*, Bouwen met Staal 103, page 3-7, SBI Rotterdam, The Netherlands, November 1993.